# Small-molecule Wnt agonists correct cleft palates in *Pax9* mutant mice *in-utero*

Shihai Jia[1], Jing Zhou[1], Christopher Fanelli[1], Yinshen Wee[1], John Bonds[2], Pascal Schneider[3], Gabriele Mues[2], Rena N. D'Souza[1,4,*]

[1]School of Dentistry and [4]Departments of Neurobiology & Anatomy, Pathology, School of Medicine, University of Utah, Salt Lake City, Utah 84112, USA.

Department of Biomedical Sciences, Texas A&M University College of Dentistry, Dallas 75246, USA.

[3]Department of Biochemistry, University of Lausanne, CH-1066 Epalinges, Switzerland.

*__Corresponding author's email address__: rena.dsouza@hsc.utah.edu

**KEY WORDS**: Pax9, Wnt, Palatogenesis, Cleft Palate, Mouse, Wnt agonist small-molecules

## Summary Statement

The functional relationship between *Pax9* and Wnt genes is important in palate formation as cleft defects in *Pax9*-deficient mice are corrected after Wnt signaling is restored *in-utero*.

**Abstract**

Clefts of the palate and/or lip are the most common among human craniofacial malformations and involve multiple genetic and environmental factors. Defects can only be corrected surgically and require complex life-long treatments. Our studies utilized the well-characterized *Pax9*$^{-/-}$ mouse model with a consistent cleft palate phenotype to test small-molecule Wnt agonist therapies. We first show that the absence of Pax9 alters the expression of Wnt pathway genes including *Dkk1* and *Dkk2*, proven antagonists of Wnt signaling. The functional interactions between Pax9 and Dkk1 is shown by the genetic rescue of secondary palate clefts in *Pax9*$^{-/-}$*Dkk1*$^{f/+}$*;Wnt1Cre* embryos. The controlled intravenous delivery of small-molecule Wnt agonists (Dkk inhibitors) into pregnant *Pax9*$^{+/-}$ mice restored Wnt signaling and led to the growth and fusion of palatal shelves as marked by an increase in cell proliferation and osteogenesis *in-utero* while other organ defects were not corrected. This work underscores the importance of Pax9-dependent Wnt signaling in palatogenesis and suggests that such a functional upstream molecular relationship can be exploited for the development of therapies for human cleft palates that arise from single gene disorders.

## Introduction

Failures in palatogenesis occur during the outgrowth, elevation, migration and fusion of palatal shelves providing the best evidence that these developmental processes are under strict molecular control (Mossey et al., 2009; Greene and Pisano, 2010). Since the sequence of events in murine palatogenesis closely resemble that seen in humans, mouse genetic models with secondary palate defects have been valuable in dissecting the signaling pathways that drive palatogenesis (Funato et al., 2015). Gene ontology reveals that more than half of the genes associated with palatal clefts in mice are transcription factors, such as, *Msx1* (Satokata and Maas, 1994; Zhang et al., 2002), *Pax9* (Peters et al., 1998; Zhou et al., 2011), *Osr2* (Lan et al., 2004), *Gbx2* (Byrd and Meyers, 2005), *Tbx22* (Pauws et al., 2009), *Tfap2A* (Brewer et al., 2004), and *Hoxa2* (Gendron-Maguire et al., 1993). Moreover, growth factor families such as TGF-ßs, Shh, Fgf, and Wnt along with membranous molecules and extracellular matrix proteins are also implicated as playing important roles in palate formation (Greene and Pisano, 2010; Funato et al., 2015). Taken together, these studies reveal that a tight interplay of gene networks and environmental risk factors regulate key molecular, cellular and tissue interactions during palate development. However, much remains to be learned about how these molecules precisely function and how such knowledge can be translated into new treatment strategies for preventing or reversing cleft conditions in humans.

Among the mouse genetic models of cleft palate that are available for study, the *Pax9*$^{-/-}$ mouse model has provided valuable insights into the mechanisms that lead to the failure of palatogenesis. Pax9 belongs to the family of paired-box DNA-binding domain containing transcription factors that play key roles in organogenesis (Stapleton et al., 1993). *Pax9*$^{-/-}$ mice consistently exhibit clefts of the secondary palate and die shortly after birth. Other phenotypic defects include: agenesis of the thymus, parathyroid glands, ultimobranchial bodies and teeth (Peters et al., 1998; Zhou et al., 2011). It has been proposed that *Pax9* is involved in molecular signaling events that control the patterning

of the anterior-posterior (AP) axis during palatal shelf outgrowth. Its control of cell proliferation and its interactions with the Bmp, Fgf and Shh pathways are hence important for expansion of the palatal shelves and their growth along the AP axis and towards the midline (Zhou et al., 2013). However, there is little known about the morphogenetic gradient that controls patterning of the palatal shelves along the buccal-lingual axis. This information is critical as the closure of palatal shelves towards the midline relies on the precise actions and interactions of genes along this axis.

In these studies we demonstrate the functionality of *Pax9*'s upstream molecular relationship with Wnt signaling during palatogenesis. Our unbiased genome-wide analyses show that the inhibitors of Wnt, namely, *Dkk1* and *Dkk2,* are significantly up regulated in *Pax9*$^{-/-}$ palatal mesenchyme along with other Wnt genes that are down regulated. Definitive evidence of the importance of *Pax9's* relationship to *Dkk1* is shown by the genetic rescue of secondary palate clefts in mice that are deficient in both *Dkk1* and *Pax9*. Furthermore, the controlled intravenous delivery of a Wnt agonist small-molecule, which specifically inhibits Dkk1, into pregnant *Pax9*$^{+/-}$ mice corrects a 100% of cleft palate defects in mutant progeny. These studies underscore the importance of Pax9-dependent Wnt signaling during palatogenesis and suggest that Wnt agonist therapies can be exploited to correct cleft palate conditions in humans that arise from single-gene defects.

## Results

### Pax9 is upstream of the Wnt signaling pathway during murine palatogenesis

We first examined the molecular consequences of *Pax9* deficiency in forming palatal shelves at E13.5 using RNASeq analyses. Our data indicate that the complete lack of *Pax9* led to more than a 1.5-fold ($P < 0.01$) change in expression of approximately 1368 genes among which the Wnt pathway genes appear strongly enriched (Table 1, left column). Significant is the higher expression of *dickkopf* genes *Dkk1* and *Dkk2,* which encode extracellular proteins that block the binding of Wnt ligands to the Lrp5/6 receptor complex. The expression of Wnt ligands *Wnt3*, *Wnt7a* and *Wnt9b* were also altered along with genes involved in Bmp, Eda, Fgf and Shh signaling (Table 1, right column).

Quantitative RT-PCR analysis (Fig.1) confirmed that the Wnt signaling pathway inhibitors, *Dkk1* and *Dkk2,* had increased 1.7 fold. In contrast, *Lef1*, *Gbx2, Hand2 and Fgf4*, genes involved in Wnt signaling as well as *Msx1* and *Msx2*, partner genes of *Pax9*, were significantly down regulated in the absence of *Pax9*. Moreover, *Tfap2b*, a member of *Ap2* family that interacts with *Cited1* during craniofacial development (Braganca et al., 2002; Knight et al., 2005) was reduced more than 2-fold in E13.5 *Pax9*$^{-/-}$ palates.

The relationship between Pax9 and the Wnt pathway was further assessed by studying the expression patterns of *Dkk1*, *Dkk2* and *Pax9* during normal palatogenesis. As shown in Fig. 2A-D, *Dkk1* and *Dkk2* expression levels increased from E13.5 to E14.5 and appear restricted to posterior palatal mesenchyme, while *Pax9* expression is stronger and present in both anterior and posterior palatal mesenchyme (Fig. 2E,F,K,L). *Dkk1* transcripts are more visible (Fig. 2G,H) but appear less abundant than *Dkk2* and *Pax9* in the posterior region (Fig. 2H,J,L). The buccal-lingual gradient of expression for *Pax9* and *Dkk2* is inversely related, with *Pax9* stronger on the buccal aspects of the palatal shelves (Fig. 2L) and *Dkk2* transcripts more localized to the lingual region (Fig. 2J). While *Pax9* expression is broader and occupied the entire palatal mesenchyme in anterior palate (Fig. 2K), low levels of *Dkk1/2* expression were visible in the anterior region (Fig. 2G,I,M,Q). Interestingly, these expression domains of *Dkk1, Dkk2* and *Pax9* in posterior palatal mesenchyme differ from that of *Msx1* which localizes to the anterior region of the palatal mesenchyme (Zhang et al., 2002; Han et al., 2009; Fuchs et al., 2010). *In-situ* hybridizations showed that expression of both Wnt inhibitors increased in *Pax9*$^{-/-}$ palatal mesenchyme (Fig. 2M-T). At E13.5, *Dkk1* expression was detected in *Pax9*$^{+/+}$ posterior palatal mesenchyme (Fig. 2H,N) while its expression had increased in the posterior palate and extended into the anterior zone of *Pax9*$^{-/-}$ palatal mesenchyme (Fig. 2O,P). *Dkk2* expression was also higher in the posterior palatal mesenchyme with a lingual to buccal gradient of distribution (Fig. 2J,R) that intensified in *Pax9*$^{-/-}$ tissues (Fig. 2T).

In order to assess whether the molecular upstream relationship between Pax9 and the Wnt pathway was functional, we generated compound mutant mice where *Dkk1*

expression was reduced in a *Pax9*-deficient background. *Pax9*$^{+/-}$*Dkk1*$^{f/+}$ embryos showed normal secondary palates (Fig. 3A,D,G) while *Pax9*$^{-/-}$*Dkk1*$^{f/+}$ littermates showed clefts in this region (Fig. 3B,E,H). In 5 of 5 *Pax9*$^{-/-}$*Dkk1*$^{f/+}$*;Wnt1Cre* compound mutant mice retrieved, a complete rescue of secondary palate clefts were noted (Fig. 3C,F,I). All 5 *Pax9*$^{-/-}$*Dkk1*$^{f/+}$*;Wnt1Cre* compound mutant mice retained a supernumerary digit (Fig. S1L) and showed significant delay in tooth development (Fig. S1C), both features representing a consistent phenotype of *Pax9*$^{-/-}$*Dkk1*$^{f/+}$ mice (Fig. S1B,K). Furthermore, agenesis of the parathyroid glands and thymus was not rescued in *Pax9*$^{-/-}$ *Dkk1*$^{f/+}$*;Wnt1Cre* compound mutant mice (Fig. S1F,I). 4 of the 5 mice in this group were retrieved at E18.5 for analysis and the remaining pup that was born did not survive postnatally.

**Small-molecule Wnt agonists correct cleft palate defects in *Pax9*$^{-/-}$ mice**

The small-molecule WAY-262611, that potentiates Wnt-β-catenin signaling by specifically inhibiting Dkk1 (Pelletier et al., 2009) was administered daily from E10.5 to E14.5, a critical developmental window during which palate initiation, shelf outgrowth and elevation occurs (Fig. 4). The delivery of 5 doses of WAY-262611 (Fig. S2A), at either 12.5 mg/kg or 25 mg/kg, into the tail veins of pregnant *Pax9*$^{+/-}$ mice resulted in fusion of the secondary palate in all (18/18) *Pax9*$^{-/-}$ pups examined. Treatment from E10.5 to E13.5 rescued the cleft phenotype, but to a lesser extent than observed with the E10.5 to E14.5 regimen (Table. 2). As disclosed in Table 2, 60% (11/18) additionally displayed complete fusion between the primary and secondary palates while 7/18 showed small residual defects in the zone of fusion of the primary and secondary palates around the 3$^{rd}$ ruga (Fig. 2B). Since *Pax9*$^{-/-}$ pups die shortly after birth, E18.5 palatal shelves with residual defects were obtained from the group treated with WAY-262611 and cultured for 3 days. As shown in Fig. S3, all palates displayed complete fusion of residual defects. This suggests that the lack of complete fusion was due to a timing delay rather than to differences in gene distribution between the primary and secondary palates.

Recent studies by (Li et al., 2017) showed partial rescue of palatal defects in 64% of *Pax9*$^{-/-}$ embryos treated from E12.5 to E14.5 using an intraperitoneal route of delivery of another small-molecule Wnt agonist, III3ca. III3ca blocks the Wnt antagonists Dkk1, Dkk2 and Dkk4 (Li et al., 2012). Here we tested effects of the daily I.V. delivery of IIIc3a to pregnant dams from E10.5 to E14.5. Results showed that this schedule of III3ca intervention resulted in closure of the secondary palate defects in 80% (12/15) of embryos of which six embryos showed residual fusion defects (Table 2).

The sample size for each treatment group were confirmed by power analysis using PASS software, version 11 (Hintze, J. (2011). PASS 11. NCSS, LLC. Kaysville, Utah, USA) provided by University of Utah Study Design and Biostatistics Center to reach power > 80%. H&E as well as Masson's trichrome stains revealed that both pharmacological interventions brought about a true correction of the secondary palatal defect and the deposition of collagen-enriched matrix in the area of the midline (Fig. 5A-P). The more detailed analyses of the molecular mechanisms underlying the correction of palatal defects was performed on tissues exposed to WAY-262611 treatment as successful outcomes reached 100% with this experimental group.

Since *Pax9* regulates *Msx1*, a transcription factor that also plays a role in palatogenesis, I.V. injections of WAY-262611 and III3ca at 25 mg/kg were given to pregnant *Msx1*$^{+/-}$ mice. Such interventions failed to rescue cleft palate defects in mutant pups (0/50) (Fig. S4). Since *Msx1* expression is spatially restricted to the anterior region of palatal mesenchyme where *Dkk1* and *Dkk2* have low expression levels, it is likely that the reactivation of Wnt signaling only influenced downstream events in posterior regions of the palate where *Pax9* is more dominantly expressed.

**The *in-utero* delivery of Wnt agonists restored growth of the palatal shelves**

Evidence that these pharmacological interventions activated Wnt signaling in palatal mesenchyme comes from the increased levels of *β-catenin* activity visible in *Pax9*$^{-/-}$ palatal mesenchyme after treatment with WAY-262611 or IIIc3a (Fig. 6A-F). RNASeq data showed increased levels of Wnt target gene expression in treated palates (Table

3).WAY-262611 had no effect on *Dkk1* and *Dkk2* mRNA levels as it acts at the protein level. Expression levels of *Gbx2* and *L1cam* genes that are downstream targets of Wnt signaling, are restored following Wnt agonist therapy as shown in Fig. 6G. Notably, *Gbx2* mutant mice have cleft palate defects while *L1cam*-deficient mice show other craniofacial defects (Byrd and Meyers, 2005). Furthermore, quantitative RT-PCR analysis showed the expression levels of endogenous *Osr2*, *Msx1* and *Bmp4*, which were significantly down-regulated in the absence of *Pax9*, were not restored after treatment with WAY-262611 (Fig. S5). This suggested that the signaling hierarchy involving *Pax9* and the Wnt pathway, while critical in posterior palatal mesenchyme, may not involve these molecules.

As detailed by Zhou et al., (2011), the targeting vector used for the generation of *Pax9*$^{-/-}$ mice contained a *frt*-flanked neo expression cassette followed by a *Myc-Osr2* cDNA inserted in intron-2 of *Pax9*. *Pax9*$^{+/-}$ mice were derived from crossings with *Ella-Cre* mice. Studies of Myc-Osr2 expression are facilitated by further crossing of *Pax9*$^{+/-}$ mice with *FLPeR* mice thus eliminating the Neo cassette resulting in expression of Myc-Osr2 (Zhou et al., 2011). Here, we performed additional experiments to rule out the possibility that WAY-262611 treatments affected transgenic *Myc-Osr2* protein and mRNA expression. Fig. S6A-D showed the absence of a translated protein product from exogenous Myc-Osr2 in both untreated and treated *Pax9*$^{+/-}$ and *Pax9*$^{-/-}$ palatal shelves. In contrast, Myc-Osr2 was clearly visible in a section through *Pax9*$^{+/-}$*;FLP* palate and tooth mesenchyme where Myc-Osr2 from the transgenic *Osr2* allele is able to be translated (Fig. S6E). *In-situ* hybridization using an *Osr2*-specific probe that detects both exogenous and endogenous *Osr2* mRNA showed stronger *Osr2* signals in *Pax9*$^{-/-}$ samples (Fig. S6G,I) as the extra knock-In *Osr2* allele was transcribed into mRNA. However, no significant differences were noted in *Osr2* mRNA expression levels when comparing untreated and treated *Pax9*$^{+/-}$ samples (Fig. S6F,H) or untreated and treated *Pax9*$^{-/-}$ samples (Fig. S6G,I). Thus, WAY-262611 treatment itself did not affect *Osr2* expression and the closure of palatal shelves following Wnt interventions cannot be attributed to transgenic *Myc-Osr2* expression.

*Pax9* deficiency lowers cell proliferation in E13.5 posterior palatal mesenchyme as seen by the significant reduction in BrdU incorporation (Zhou et al., 2013). BrdU assays were performed in WAY-262611 treated embryos at both E13.5 and E14.5 stages when palatal outgrowth is most visible. After treatment with WAY-262611, cell proliferation was restored to a level that appeared adequate for the outgrowth of palatal shelves (Fig. 7A-G). The BrdU labeling assay in posterior palate at E14.5 showed that the ratios of BrdU positive palatal mesenchymal cells were significantly reduced in the *Pax9*$^{-/-}$ samples (Fig. 7E,F) confirming previous reports (Zhou et al., 2013). After Wnt signaling agonist treatments, the ratios of BrdU positive palatal mesenchymal cells were consistently restored in *Pax9*$^{-/-}$ samples at both E13.5 and E14.5 (Fig. 7B,D) when compared to *Pax9*$^{+/-}$ tissues (Fig. 7A,C,G).

To better understand whether the closure of *Pax9*$^{-/-}$ palatal shelves following Wnt agonist treatment had palatine bone formation, we compared alkaline phosphatase activity and type I collagen (*Col1a1*) mRNA expression in treated and untreated *Pax9*$^{+/+}$ and *Pax9*$^{-/-}$ maxillary and palatine processes. The robust levels of enzymatic activity observed in treated *Pax9*$^{-/-}$ tissues closely resembled that in *Pax9*$^{+/+}$ tissues and showed the onset of osteogenesis in these areas (Fig. 8A-F). Alkaline phosphatase activity that marks early osteoblast differentiation was activated in areas of mesenchymal condensations at osteogenic fronts within palatal mesenchyme at E15.5 in *Pax9*$^{+/+}$ embryos (Fig. 8A,D). However, alkaline phosphatase activity was not detected in stunted *Pax9*$^{-/-}$ palatal shelves (Fig. 8B,E). After Wnt agonist treatment, enzymatic activity was restored in the *Pax9*$^{-/-}$ palate (Fig. 8C,F). *Col1a1,* a marker of differentiated osteoblasts appeared in osteoblasts in *Pax9*$^{+/+}$ palatal mesenchyme. In contrast, *Pax9*$^{-/-}$ samples failed to show *Col1a1* expression in putative mesenchyme. After Wnt agonist treatment, *Col1a1* expression was restored as indicated by the osteogenic activity within the palatal shelves (Fig. 8G-X).

Taken together, these data establish that the I.V. delivery of small-molecule Wnt agonists to pregnant *Pax9*$^{+/-}$ females within a critical gestational window was effective in bringing about true closure of the palatal shelves in *Pax9*$^{-/-}$ embryos (Figs. 5,8). While

Wnt signaling was restored in treated palates, Wnt agonist therapies did not correct the developmental arrest of tooth organs, parathyroid glands, thymus and hind limb defects in treated mutants (Fig. S7). Neither did the Wnt therapy lead to prolonged survival of treated *Pax9*$^{-/-}$ neonates, suggesting that the cleft palate was not the only defect causing *Pax9*$^{-/-}$ neonates dead after birth. The MRI imaging showed that *Pax9*$^{+/-}$ mothers injected with WAY-262611 along with their wild type and heterozygous progeny, showed no toxic effects or tumor development up to 18 months following the last tail-vein injection (Data not shown).

## Discussion

In these studies, we provide definitive evidence that *Pax9* deficiency alters Wnt activity in palatal shelves and that this upstream relationship, when genetically restored, leads to the rescue of the cleft palate phenotype in *Pax9*$^{-/-}$ embryos. Of significance is the high fidelity correction of palatal defects in *Pax9*$^{-/-}$ embryos after the controlled I.V. delivery of small-molecule Dkk inhibitors (Wnt agonists) to pregnant *Pax9*$^{+/-}$ mice during a critical developmental window for palatogenesis. Such interventions restored Wnt signaling in palatal mesenchyme and specifically increased cell proliferation within posterior palatal mesenchyme where *Pax9* and *Dkks* have inverse expression patterns. Wnt activation in *Pax9*$^{-/-}$ palates led to a true bony closure of palatal shelves through osteogenesis. Collectively, these data demonstrate that the Pax9/Wnt pathway is critical for the formation of the secondary palate and that restoring this molecular equilibrium in *Pax9*$^{-/-}$ mice *in-utero* leads to the complete fusion of palatal shelves.

### Pax9-dependent Wnt signaling along the buccal-lingual axis is important for palate development

Our studies demonstrate that Pax9-dependent Wnt signaling in the posterior domain of palatal mesenchyme influences growth along the buccal - lingual axis thus providing new insights into the molecular mechanisms underlying Pax9's actions in palatogenesis. The inverse or complementary patterns of *Pax9* and *Dkk1/Dkk2* gene expression in posterior mesenchyme suggests that Pax9 modulates Wnt signaling in this region of the

palate. Our unbiased studies of genome-wide alterations in whole *Pax9*$^{-/-}$ palatal shelves, showed a significant increase in *Dkk1* and *Dkk2* expression. Genes involved in other signaling pathways such as *Msx1* and *Bmp4* were also altered. Since these genes influence signaling events in anterior palatal mesenchyme this explains why Wnt agonist therapy did not result in closure of palatal defects in *Msx1*$^{-/-}$ mice. We also conclude that *Pax9*-dependent Wnt signaling through the control of *Dkk1* expression is key for posterior palate formation. Our expression analyses supports the results of studies by Li et al., (2017) that show the restriction of *Axin2* and *ß-catenin* to the posterior region of the palate and that these genes are down regulated in the absence of *Pax9* while *Dkk2* levels increase in posterior palatal mesenchyme. Notably, the expression levels of selective Wnt ligands were reduced in the absence of *Pax9* and were not normalized after activation of Wnt signaling. Earlier studies have shown that *Dkk* expression can be regulated by Wnt-induced TCF activation through a negative feedback mechanism (Niida et al., 2004). Hence, it will be interesting to explore whether Pax9 directly regulates the expression of Wnt ligands themselves.

Notably, Pax9's role in regulating the Wnt signaling pathway through its inhibition of *Dkk1* suggests that it serves dual transcriptional functions in palatogenesis. As an activator of Bmp and Fgf signaling in anterior palatal mesenchyme and as a likely repressor of *Dkk1* functions in posterior mesenchyme, Pax9 influences patterning morphogenesis throughout the forming palate. The literature underscores the role of Pax family members as transcriptional regulators that act as activators and repressors during development. For example, *Pax6*, has dual roles in eye development (Duncan et al., 1998), as it serves as an activator of the *αA*-, *αB*- and *δ1-crystallin* genes while repress the expression of *β-crystallin* gene in the lens. Pax4 also acts as a transcriptional repressor in the pancreas (Fujitani et al., 1999). It is well established that Pax9 is involved in the formation of pharyngeal organs (thymus, parathyroid) as well as tooth and palate development. Pax9 activates the Bmp and Fgf signaling pathways (Mensah et al., 2004) during tooth development but is strongly synergistic with BF-1 (brain factor-1) and the potent breast cancer-associated transcriptional repressor, PLU-1 (Tan et al., 2003). Hence, Pax9's functions in the development of craniofacial and

pharyngeal pouch derivatives are the result of the fine-tuned modulations of its multiple transcriptional properties.

While it can be argued that relief of Dkk1 inhibition could overcome reduced Wnt signaling activity at some other point in the pathway, the rescue of the cleft palate defect in *Pax9*$^{-/-}$*Dkk1*$^{f/+}$*;Wnt1Cre* compound mutant mice as shown here, suggests that the functional relationship of *Pax9* with *Dkk1* is both necessary and sufficient for palate shelf closure. Reports by Li et al., (2017) indicate that secondary palate clefts are rescued in 14 out of 20 double mutants that lack *Wise*, another secreted Wnt ligand-receptor antagonist that also modulates Bmp signaling. Confounding is the observation that in the absence of *Pax9*, expression levels of *Wise*, are down regulated in palatal shelves. Our studies provide definitive evidence that Pax9's role in regulating the Wnt signaling pathway through its inhibition of Dkk1 is one means by which it exerts its modulatory functions in patterning morphogenesis. Clearly, the relationship with other Wnt signaling molecules and pathways such as Bmp and Fgf signaling also play a role in processes that drive palatogenesis.

**The correction of *Pax9*-mediated palatal defects with Wnt agonists underscores the importance of this molecular pathway in secondary palate formation**

The surprising fidelity with which palatal defects are corrected in *Pax9*$^{-/-}$ embryos, through the controlled intravenous delivery of Wnt agonists can be explained by the fact that Wnt signaling genes are potent downstream effectors of Pax9's functions in palatal mesenchyme. Interestingly, such interventions could not restore the development of the thymus, parathyroid glands, and ultimobranchial bodies or correct other defects such as supernumerary preaxial digits. It is likely that organs other than the secondary palate, that are derived from the pharyngeal pouches may require essential contributions from other downstream effector pathways such as Bmp, Fgf and Shh. Alternatively, Wnt agonist delivery and dosage schedules that proved optimal for palatogenesis would have to be modified to achieve the correction of other organ defects in *Pax9*$^{-/-}$ mice.

The interventions with small molecule Wnt agonists failed to prolong the survival of *Pax9*$^{-/-}$ neonate pups from treated pregnant dams as they succumb at birth. While earlier studies have noted that *Pax9*$^{-/-}$ newborn pups die shortly at birth, most likely as a consequence of secondary palate clefts (Peters et al., 1998), our data suggest that systemic alterations caused by the absence of parathyroids and thymus glands may lead to early death.

It is intriguing that Wnt agonists when delivered intravenously during a critical developmental window for odontogenesis, only advanced tooth organs to the early cap stage. In humans, mutations in *PAX9* are mainly associated with congenitally missing posterior teeth (Goldenberg et al., 2000; Stockton et al., 2000). *Pax9* also influences epithelial-mesenchymal signaling events that drive murine tooth morphogenesis (Peters et al., 1998; Nakatomi et al., 2010). Mutations in *WNT10A* account for the majority of human tooth agenesis cases (Bohring et al., 2009; van den Boogaard et al., 2012; Mues et al., 2014) and canonical Wnts are key drivers of tooth signaling interactions likely to be downstream of *Pax9* in dental mesenchyme (O'Connell et al., 2012; Jia et al., 2016). *Pax9* also integrates dental mesenchymal signaling events that involve *Bmp4*, *Fgf3* or *Fgf10* (Peters et al., 1998; Nakatomi et al., 2010). Hence, combinatorial therapies involving Wnt agonists and these growth factors may prove more effective in advancing tooth morphogenesis and should be the focus of future studies.

We also observed that the intravenous delivery of Wnt agonist small-molecules failed to rescue cleft defects in 50 *Msx1*$^{-/-}$ mice. *Msx1* is a partner gene of *Pax9* that also plays a role in palatogenesis and is more dominantly expressed in the anterior zone of palatal mesenchyme. In contrast, *Pax9* and the *Dkks* are more restricted to the posterior region. We hypothesize that a morphogenetic gradient of differential gene expression along the anterior-posterior axis controls the patterning and closure of palatal shelves (Hilliard et al., 2005; Zhou et al., 2013) and that downstream effector genes other than the Wnts are likely to mediate *Msx1*'s actions in anterior palatal mesenchyme.

**Clinical implications for the use of small-molecule replacement therapies for the treatment of developmental disorders of the craniofacial complex**

The wide implications of the Wnt-ß-catenin signaling pathway in many developmental processes and in adult tissue homeostasis has encouraged development of pharmacological modulators of this pathway (Clevers and Nusse, 2012; Baron and Kneissel, 2013; Kahn, 2014). Previously, a small-molecule-based chemical genetic approach restored the stability and function of GSK-3ß in *GSK-3ß*$^{FRB*/FRB*}$ mice, such that after rapamycin treatment, cleft defects were rescued in 6 of 9 mutant pups (Liu et al., 2007). New therapies that block the function of the Wnt antagonist, *sclerostin*, restored bone mass and strength in humans at risk for fractures (Recker et al., 2015). Several preclinical studies also report that other therapies targeting Dkk1 inhibition induce bone gain (Baron and Kneissel, 2013).

Our data indicate that the intravenous administration of small-molecule Dkk inhibitors increased Wnt signaling in palatal mesenchyme and enhanced cell proliferation, palatal shelf outgrowth and fusion. Restoration of cell proliferation during a critical developmental window, when expansion of the cranium can force shelves apart, appears critical for palate formation. In humans, sub-mucosal clefting occurs as commonly as overt cleft palate and is the result of apposition of overlying soft tissue with a lack of palatal bone formation (Garcia Velasco et al., 1988). For this reason, it was important for us to first demonstrate that Wnt agonist therapies did positively affect palate morphogenesis (as shown by increased cell proliferation) and that this was sufficient for osteogenesis to ensue within the palatal shelves. Further studies are needed to delineate stage-specific effects of Wnt agonist therapies and the role of Pax9-dependent Wnt signaling in palatal shelf growth and bone formation.

Questions naturally arise about how such approaches can be translated into therapies for human cleft palate disorders. Since Wnt signaling is key to the development of several organs, activation of the pathway through exogenous Wnt agonist therapies

could lead to abnormalities in other organ systems. Our histopathologic and MRI imaging analyses of pregnant *Pax9*$^{+/-}$ females that received Wnt agonist injections and surviving *Pax9*$^{+/+}$ or *Pax9*$^{+/-}$ littermates showed no toxic effects or tumor development up to 18 months following the last tail-vein injection. Hence, small doses of Wnt agonists that target inhibitors of receptor binding when delivered in a controlled manner and during a specific developmental window only affect cells like those in the palatal mesenchyme that have not reached threshold levels needed for the hierarchy of Wnt signaling.

Although ultrasound technologies can diagnose cleft palate conditions as early as 13 weeks of gestation, small-molecule therapies delivered in low doses to pregnant mothers are likely to be fraught with difficulties and will require further experimentation on risk to benefit ratios. Alternate strategies to reduce exposure of the mother could include delivery into the amniotic fluid as shown to be effective for the delivery of recombinant ectodysplasin (Hermes et al., 2014). Alternatively, early postnatal interventions that utilize the well-timed local delivery of Wnt agonist small-molecules or proteins during surgical correction procedures may prove effective in bringing about the timely closure of palatal shelves.

## Materials and Methods

### Animals

All animal procedures were approved by the Institutional Animal Care and Use Committee (IACUC) at the University of Utah (Protocol #17-02004). *Pax9*$^{+/-}$ and *Msx1*$^{+/-}$ mice were provided by Dr. Rulang Jiang (Cincinnati Children's Hospital) (Zhou et al., 2011) and Dr. Yiping Chen (Tulane University). Whole heads of E13.5 and E14.5 *Dkk1*$^{Tg107\text{-}LacZ}$ embryos were provided by Dr. Ulrich Rüther (Heinrich-Heine-University) (Lieven et al., 2010). *BAT-Gal* mice for studies on Wnt activity (Maretto et al., 2003) and *FLP* male mice for the generation of positive control Myc-Osr2 (JAX 016226) were purchased from Jackson Laboratories. The *Pax9*$^{+/-}$, *Msx1*$^{+/-}$ and *BAT-Gal* mice were maintained in *C57BL/6* background. 2 to 8 month-old females were used for intercross

matings and adult mice, over 18 months of age, were used for the histopathologic and Magnetic Resonance Imaging (MRI) analysis of potential side effects and toxicity following treatments. We were diligent in including litter-matched controls that were subject to the same Wnt agonist therapy *in-utero*. However, since some litters failed to yield *Pax9*$^{+/+}$ progeny, *Pax9*$^{+/-}$ littermates were used instead as it is well documented that Pax9 haplo-insufficiency does not compromise the development or functions of any organ system (Peters et al., 1998; Zhou et al., 2011).

*Pax9*$^{-/-}$*Dkk1*$^{f/+}$*;Wnt1Cre* compound mutant mice were generated through serial matings. *Pax9*$^{+/-}$ mice were first mated with *Dkk1*$^{f/+}$ mice (EM: 09872 from EMMA mouse repository) to generate *Pax9*$^{+/-}$*Dkk1*$^{f/+}$ progeny. We next mated *Pax9*$^{+/-}$*Dkk1*$^{f/+}$ with *Wnt1Cre* (JAX 022501, Jackson Laboratory) to generate *Pax9*$^{+/-}$*Dkk1*$^{f/+}$*;Wnt1Cre* males. *Pax9*$^{-/-}$*Dkk1*$^{f/+}$*;Wnt1Cre* embryos were then obtained from the mating of *Pax9*$^{+/-}$ *Dkk1*$^{f/+}$*;Wnt1Cre* males with *Pax9*$^{+/-}$*Dkk1*$^{f/+}$ females.

**Palatal dissections, RNASeq and quantitative RT-PCR**

The embryos were harvested at E13.5 and heads collected in cold PBS. After the lower jaw and brain were removed under a dissecting microscope, the status of the palatal shelves was evaluated. Palatal tissues were carefully dissected using fine forceps, quickly frozen in liquid nitrogen and stored individually at -80°C for total RNA extraction (Zhou et al., 2013; Kim et al., 2017).

Whole transcriptome profiling of developing palatal shelves was performed by RNASeq as previously described (Jia et al., 2013). Sequenced reads were mapped to the reference mouse genome (mm10) using Novoalign (v2.08.03). Read counts were generated using USeq's Defined Region Differential Seq application and normalized counts were used in DESeq2 to measure differential expression. The RNASeq raw data have been deposited into Gene Expression Omnibus database (GEO) (http://www.ncbi.nlm.nih.gov/geo) under accession number GSE89603 and GSE101825. The candidate genes were screened from a comparison of 5 sets of data as follows: First, the normalized counts were cut-off at 10 in at least one of the samples, then the

fold change was chosen at 1.5-fold or higher and at *P*-values <0.01 from the Audic Claverie test with Benjamini Hochberg FDR multiple testing correction. Next, the gene list was sorted by *P*-value and lists of genes were submitted to DAVID (https://david.ncifcrf.gov) or Toppgene (https://toppgene.cchmc.org) for functional enrichment analysis.

Palatal shelves were micro-dissected from E13.5 embryos. After genotyping, total RNA was extracted from individual samples using the RNeasy Micro Kit (Qiagen). First-strand cDNA was synthesized using the SuperScript First-Strand Synthesis System IV (Thermo Fisher Scientific). Quantitative RT-PCRs were performed in a StepOnePlus$^{TM}$ Real-Time PCR System (Applied Biosystems) using the SYBR Green$^{ER}$ qPCR Supermix (Thermo Fisher Scientific). A list of gene-specific primers is provided in the Table S1. For each sample, the relative levels of target mRNAs were normalized to *Gapdh* using the standard curve method. 5 sets of replicates were analyzed for each gene.

**Delivery of Small-Molecule Wnt Pathway agonists**

Two small-molecules agonists purchased from Millipore (Billerica, MA, USA) were used to treat the timed pregnant female mice. WAY-262611, (1-(4-(Naphthalen-2-yl)pyrimidin-2-yl)piperidin-4-yl)methanamine, is a 2-aminopyrimidine compound (Fig. S2A) that antagonizes the effect of Dkk-1 by preventing the formation of the Dkk1/LRP5/Kr2 complex. It has a half-life ($t_{1/2}$) of 6-8 hours in plasma (Pelletier et al., 2009) and specifically inhibits Dkk1 at $EC_{50}$=0.63 µM, based on a TCF-luciferase assay. IIIc3a, 9-Carboxy-3-(dimethyliminio)-6,7-dihydroxy-10-methyl-3H-phenoxazin-10-iumiodide, is an enhanced in-solution stable gallocyanine analog (Fig. S2B) that disrupts the interaction of LRP5/6 with Dkks 1,2, and 4 (Dickkopf) in a competitive manner at $EC_{50}$=5 µM in LEF-luciferase assay using NIH3T3 cells (Li et al., 2012). Stock solutions of WAY-262611 and IIIc3a were prepared at 25 mg/ml in DMSO. Dilutions at 12.5 and 25 mg/kg per mouse body weight were prepared prior to injection into the tail vein as previously described (Kowalczyk et al., 2011). Control treatments consisted of tail-vein injections of 10% DMSO in PBS. Injections of WAY-262611 and III3ca were delivered separately

each day from E10.5 to E14.5 while an additional group of mice received WAY-262611 treatments from E10.5 to E13.5 as detailed in Table 2. Mice were closely monitored for any discomfort or side effects.

**Microscopic evaluations and *in-situ* hybridizations**

Embryos retrieved from treated and untreated litters were immediately fixed in 4% paraformaldehyde (PFA) overnight. 7 µm-thick paraffin sections were prepared and stained with hematoxylin and eosin (H&E) for microscopic evaluation. *In-situ* hybridizations were performed using digoxigenin-labeled RNA probes to *Dkk1*, *Dkk2, Pax9, Osr2* and *Col1a1* as described previously (D'Souza et al., 1993; Zhang et al., 1999). 1 µg/ml antisense RNA probe was loaded on each section and anti-digoxigenin-AP antibody (11093274910, ROCHE, 1:1000) was used to detect the labeled probe. The BM-purple (11442074001, ROCHE) was used for color development. Comparable images were captured on a digital microscope (EVOS). For whole-mount *in-situ* hybridizations, a 2 µg/ml antisense RNA probe was loaded on each sample and anti-digoxigenin-AP antibody (11093274910, Roche, 1:2000) was used to detect the labeled probe. NTMT buffer with 4.5 µl/ml nitroblue tetrazolium (NBT) and 3.5 µl/ml 5-bromo-4-chloro-3-indolyl phosphate (BCIP) was used for color development. Adding both NBT and BCIP helped enhance the development of the reaction. For each assay, at least 5 replicates were performed.

**Gross examinations, histopathologic and MRI analyses**

All mouse embryos, neonates and adults were first evaluated through full-body visual examination. Whole embryos were fixed in 10% neutral buffered formalin, 7 µm-thick transverse paraffin sections were stained with H&E for microscopic evaluation. $Pax9^{-/-}$ embryos from treated and control litters were easily identifiable due to the supernumerary hind limb digit. However, genotyping was performed on all animals. Adult mice were anaesthetized with isoflurane and fixed by whole-body perfusion prior to magnetic resonance imaging (MRI) that was performed using 7 Tesla Bruker BioSpec MRI scanner under the following parameters: A T2 weighted RARE scan was acquired

using a 7.2 cm-diameter quadrature radiofrequency transmitter-receiver (Bruker Biospec), with 125 µm isotropic resolution, echo train length of 4, matrix size of 768x256x256 and TE/TR = 41/1200 ms on a Bruker Biospec 70/30 instrument (Bruker Biospin, Ettlingen, Germany).

**Histochemical and immunofluorescent staining procedures**

For whole mount LacZ staining, the embryos were fixed in 1% PFA then treated as previously described (Lan et al., 2004). In addition, serial coronal sections were stained with Masson's trichrome (Chen et al., 2009) to evaluate connective tissue deposition. For alkaline phosphatase (ALP) staining, embryos were fixed in 4% paraformaldehyde overnight. The frozen sections were incubated in the NTMT buffer (100 mM NaCl, 100 mM Tris–HCl pH 9.5, 50 mM MgCl2, 0.1% Tween-20) containing 4.5 µl/ml nitroblue tetrazolium (NBT) and 3.5 µl/ml 5-bromo-4-chloro-3-indolyl phosphate (BCIP) for 20 min RT (Baek et al., 2011). Comparable images were taken with a digital microscope (EVOS) or a stereomicroscope (Zeiss Stemi 508). For each assay, at least 5 replicates were used to establish reproducibility of results.

For immunofluorescent staining, embryos were fixed in 4% paraformaldehyde overnight at 4ºC and processed for paraffin sections with a thickness of 7 µm. Indirect immunofluorescent staining was performed as described (Zhou et al., 2011). After blocking with PBS containing 10% goat serum, 2% BSA and 0.1% Tween-20, overnight incubation with monoclonal anti-Myc antibody (Millipore Corporation, #05-724, 1:100 in blocking solution) was carried out at 4°C. The secondary antibody used was the goat anti-mouse IgG, Alexa Fluor 594 (Thermo Fisher Scientific, #R37121, 1:1000 in blocking solution).

**BrdU labeling and cell proliferation assay**

As reported, palatal cell proliferation was decreased in *Pax9*$^{-/-}$ embryos as early as E13.5 (Zhou et al., 2013) and contributes to the failure of shelf outgrowth. Important for these studies is the observation that daily delivery of WAY-262611 from E10.5 to E14.5 (5 days) resulted in 100% palate closure in *Pax9*$^{-/-}$ embryos while the incidence of

palatal shelf fusion was reduced when drug delivery was stopped a day earlier at E13.5. Hence, we analyzed E13.5 palatal shelves along with E14.5 palatal shelves to assess the effects of Wnt agonist therapy on cell proliferation at a critical phase of palatogenesis.

Timed pregnant female mice were injected once intraperitoneally at E13.5 and E14.5 with the BrdU Labeling Reagent (Roche, 15 µl/g body weight). Embryos were harvested two hours later. 7-µm paraffin sections were prepared in the coronal plane and spanning the entire posterior region of the palatal shelves. After rehydration, proteinase K digestion was followed by HCl treatment and incubation in a blocking solution (2% BSA, 10% goat serum, 0.1% Tween in PBS). Samples were treated with Alexa Fluor 594-conjugated anti-BrdU antibody (Thermo Fisher Scientific, #B35132) solution (1:50 in blocking solution) overnight. After counterstain with Hoechst, images were obtained from 20 sections per tissue sample using a Nikon fluorescence microscope and analyzed with Imaris software. The cell proliferation data were recorded and analyzed from 5 independent control and mutant littermate pairs.

**Whole palate shelf organ culture**

The WAY-262611 treated palates were dissected on ice by removing the lower jaw and brain and samples with residual fusion defects were marked and cultured as previously described (Almaidhan et al., 2014). *Pax9*$^{+/-}$ and untreated *Pax9*$^{-/-}$ embryos were cultured as controls. The dissected E18.5 palate shelves were put into 2 ml of medium (CO2 independent medium, Thermo Fisher Scientific, #18045-088; 20% FBS; 1X antimycotic-antibiotic, Thermo Fisher Scientific #15240-096). Culture tubes were rotated 12 rpm at an angle of 20 degree in a 37°C incubator for 3 days with daily media changes. After pictures were taken with a stereomicroscope, tissues were fixed and embedded for histologic analyses. At least 5 replicates of each treatment and genotype were utilized for culture experiments.

## Acknowledgments

We are grateful to Dr. Jeffrey Pelletier for sharing his insights on the use of WAY-262611 and the technical assistance of Mr. Greg Pratt. The following grants from the National Institutes of Health supported this research: DE019471 (including an ARRA supplement) and DE027255 to R.D.S; DE019554 to G.M. and a training stipend from DE018380 (PI - R.D.S.) to J.B. P.S. is supported by grants from the Swiss National Science Foundation.

## Competing Interests

The authors declare no competing financial interests.

## Author contributions

S.J. designed and performed RNASeq and hybridization experiments, mouse tail-vein injections and breeding. He also carried out data analysis, prepared the figures and contributed to manuscript writing; J.Z. performed BrdU staining and counts, histology analysis, quantitative RT-PCR assays as well as whole-mount hybridizations; C.F. prepared histologic sections and assisted with animal injections, alkaline phosphatase staining and *in-situ* hybridizations as part of his dental student summer research project; Y.W. prepared the samples for MRI and assisted with quantitative RT-PCR assays and BrdU positive cell counting; J.B. performed the initial round of small-molecule Wnt agonist therapy as part of his Ph.D. dissertation project; P.S. provided crucial guidance in the design of these experiments and contributed comments on the manuscript along with G.M. who helped conceive the study with R.D.S. All experiments were designed and data analyzed by R.D.S. who wrote the manuscript.

## Funding

The following grants from the National Institutes of Health have supported this research: DE019471, DE019471-ARRA supplement and DE027255 to R.D.S; DE019554 to G.M. and a training stipend from DE018380 (PI - R.D.S.) to J.B. P.S. is supported by grants from the Swiss National Science Foundation.

## Data availability

The RNASeq raw data have been deposited into NCBI Gene Expression Omnibus database (GEO) (http://www.ncbi.nlm.nih.gov/geo) under accession number GSE89603 and GSE101825. All material requests and correspondence should be addressed to R.D.S. (rena.dsouza@hsc.utah.edu)

## References


**Almaidhan, A., Cesario, J., Landin Malt, A., Zhao, Y., Sharma, N., Choi, V. and Jeong, J.** (2014). Neural crest-specific deletion of Ldb1 leads to cleft secondary palate with impaired palatal shelf elevation. *BMC Dev Biol* **14**, 3.

**Baek, J. A., Lan, Y., Liu, H., Maltby, K. M., Mishina, Y. and Jiang, R.** (2011). Bmpr1a signaling plays critical roles in palatal shelf growth and palatal bone formation. *Dev Biol* **350**, 520-531.

**Baron, R. and Kneissel, M.** (2013). WNT signaling in bone homeostasis and disease: from human mutations to treatments. *Nat Med* **19**, 179-192.

**Bohring, A., Stamm, T., Spaich, C., Haase, C., Spree, K., Hehr, U., Hoffmann, M., Ledig, S., Sel, S., Wieacker, P. and Ropke, A.** (2009). WNT10A mutations are a frequent cause of a broad spectrum of ectodermal dysplasias with sex-biased manifestation pattern in heterozygotes. *Am J Hum Genet* **85**, 97-105.

**Braganca, J., Swingler, T., Marques, F. I., Jones, T., Eloranta, J. J., Hurst, H. C., Shioda, T. and Bhattacharya, S.** (2002). Human CREB-binding protein/p300-interacting transactivator with ED-rich tail (CITED) 4, a new member of the CITED family, functions as a co-activator for transcription factor AP-2. *J Biol Chem* **277**, 8559-8565.

**Brewer, S., Feng, W., Huang, J., Sullivan, S. and Williams, T.** (2004). Wnt1-Cre-mediated deletion of AP-2alpha causes multiple neural crest-related defects. *Dev Biol* **267**, 135-152.

**Byrd, N. A. and Meyers, E. N.** (2005). Loss of Gbx2 results in neural crest cell patterning and pharyngeal arch artery defects in the mouse embryo. *Dev Biol* **284**, 233-245.

**Chen, J., Lan, Y., Baek, J. A., Gao, Y. and Jiang, R.** (2009). Wnt/beta-catenin signaling plays an essential role in activation of odontogenic mesenchyme during early tooth development. *Dev Biol* **334**, 174-185.

**Clevers, H. and Nusse, R.** (2012). Wnt/beta-catenin signaling and disease. *Cell* **149**, 1192-1205.

**D'Souza, R. N., Niederreither, K. and de Crombrugghe, B.** (1993). Osteoblast-specific expression of the alpha 2(I) collagen promoter in transgenic mice: correlation with the distribution of TGF-beta 1. *J Bone Miner Res* **8**, 1127-1136.

**Duncan, M. K., Haynes, J. I., 2nd, Cvekl, A. and Piatigorsky, J.** (1998). Dual roles for Pax-6: a transcriptional repressor of lens fiber cell-specific beta-crystallin genes. *Mol Cell Biol* **18**, 5579-5586.

**Fuchs, A., Inthal, A., Herrmann, D., Cheng, S., Nakatomi, M., Peters, H. and Neubuser, A.** (2010). Regulation of Tbx22 during facial and palatal development. *Dev Dyn* **239**, 2860-2874.

**Fujitani, Y., Kajimoto, Y., Yasuda, T., Matsuoka, T. A., Kaneto, H., Umayahara, Y., Fujita, N., Watada, H., Miyazaki, J. I., Yamasaki, Y. and Hori, M.** (1999). Identification of a portable repression domain and an E1A-responsive activation domain in Pax4: a possible role of Pax4 as a transcriptional repressor in the pancreas. *Mol Cell Biol* **19**, 8281-8291.

**Funato, N., Nakamura, M. and Yanagisawa, H.** (2015). Molecular basis of cleft palates in mice. *World J Biol Chem* **6**, 121-138.

**Garcia Velasco, M., Ysunza, A., Hernandez, X. and Marquez, C.** (1988). Diagnosis and treatment of submucous cleft palate: a review of 108 cases. *Cleft Palate J* **25**, 171-173.

**Gendron-Maguire, M., Mallo, M., Zhang, M. and Gridley, T.** (1993). Hoxa-2 mutant mice exhibit homeotic transformation of skeletal elements derived from cranial neural crest. *Cell* **75**, 1317-1331.

**Goldenberg, M., Das, P., Messersmith, M., Stockton, D. W., Patel, P. I. and D'Souza, R. N.** (2000). Clinical, radiographic, and genetic evaluation of a novel form of autosomal-dominant oligodontia. *J Dent Res* **79**, 1469-1475.

**Greene, R. M. and Pisano, M. M.** (2010). Palate morphogenesis: current understanding and future directions. *Birth Defects Res C Embryo Today* **90**, 133-154.

**Han, J., Mayo, J., Xu, X., Li, J., Bringas, P., Jr., Maas, R. L., Rubenstein, J. L. and Chai, Y.** (2009). Indirect modulation of Shh signaling by Dlx5 affects the oral-nasal patterning of palate and rescues cleft palate in Msx1-null mice. *Development* **136**, 4225-4233.

**Hermes, K., Schneider, P., Krieg, P., Dang, A., Huttner, K. and Schneider, H.** (2014). Prenatal therapy in developmental disorders: drug targeting via intra-amniotic injection to treat X-linked hypohidrotic ectodermal dysplasia. *J Invest Dermatol* **134**, 2985-2987.

**Hilliard, S. A., Yu, L., Gu, S., Zhang, Z. and Chen, Y. P.** (2005). Regional regulation of palatal growth and patterning along the anterior-posterior axis in mice. *J Anat* **207**, 655-667.

**Jia, S., Kwon, H. E., Lan, Y., Zhou, J., Liu, H. and Jiang, R.** (2016). Bmp4-Msx1 signaling and Osr2 control tooth organogenesis through antagonistic regulation of secreted Wnt antagonists. *Dev Biol* **420**, 110-119.

**Jia, S., Zhou, J., Gao, Y., Baek, J. A., Martin, J. F., Lan, Y. and Jiang, R.** (2013). Roles of Bmp4 during tooth morphogenesis and sequential tooth formation. *Development* **140**, 423-432.

**Kahn, M.** (2014). Can we safely target the WNT pathway? *Nat Rev Drug Discov* **13**, 513-532.

**Kim, S., Prochazka, J. and Bush, J. O.** (2017). Live Imaging of Mouse Secondary Palate Fusion. *J Vis Exp*.

**Knight, R. D., Javidan, Y., Zhang, T., Nelson, S. and Schilling, T. F.** (2005). AP2-dependent signals from the ectoderm regulate craniofacial development in the zebrafish embryo. *Development* **132**, 3127-3138.

**Kowalczyk, C., Dunkel, N., Willen, L., Casal, M. L., Mauldin, E. A., Gaide, O., Tardivel, A., Badic, G., Etter, A. L., Favre, M., Jefferson, D. M., Headon, D. J., Demotz, S. and Schneider, P.** (2011). Molecular and therapeutic characterization of anti-ectodysplasin A receptor (EDAR) agonist monoclonal antibodies. *J Biol Chem* **286**, 30769-30779.

**Lan, Y., Ovitt, C. E., Cho, E. S., Maltby, K. M., Wang, Q. and Jiang, R.** (2004). Odd-skipped related 2 (Osr2) encodes a key intrinsic regulator of secondary palate growth and morphogenesis. *Development* **131**, 3207-3216.

**Li, C., Lan, Y., Krumlauf, R. and Jiang, R.** (2017). Modulating Wnt Signaling Rescues Palate Morphogenesis in Pax9 Mutant Mice. *J Dent Res*, 22034517719865.

**Li, X., Shan, J., Chang, W., Kim, I., Bao, J., Lee, H. J., Zhang, X., Samuel, V. T., Shulman, G. I., Liu, D., Zheng, J. J. and Wu, D.** (2012). Chemical and genetic evidence for the involvement of Wnt antagonist Dickkopf2 in regulation of glucose metabolism. *Proc Natl Acad Sci U S A* **109**, 11402-11407.

**Lieven, O., Knobloch, J. and Ruther, U.** (2010). The regulation of Dkk1 expression during embryonic development. *Dev Biol* **340**, 256-268.

**Liu, K. J., Arron, J. R., Stankunas, K., Crabtree, G. R. and Longaker, M. T.** (2007). Chemical rescue of cleft palate and midline defects in conditional GSK-3beta mice. *Nature* **446**, 79-82.

**Maretto, S., Cordenonsi, M., Dupont, S., Braghetta, P., Broccoli, V., Hassan, A. B., Volpin, D., Bressan, G. M. and Piccolo, S.** (2003). Mapping Wnt/beta-catenin signaling during mouse development and in colorectal tumors. *Proc Natl Acad Sci U S A* **100**, 3299-3304.

**Mensah, J. K., Ogawa, T., Kapadia, H., Cavender, A. C. and D'Souza, R. N.** (2004). Functional analysis of a mutation in PAX9 associated with familial tooth agenesis in humans. *J Biol Chem* **279**, 5924-5933.

**Mossey, P. A., Little, J., Munger, R. G., Dixon, M. J. and Shaw, W. C.** (2009). Cleft lip and palate. *Lancet* **374**, 1773-1785.

**Mues, G., Bonds, J., Xiang, L., Vieira, A. R., Seymen, F., Klein, O. and D'Souza, R. N.** (2014). The WNT10A gene in ectodermal dysplasias and selective tooth agenesis. *Am J Med Genet A* **164A**, 2455-2460.

**Nakatomi, M., Wang, X. P., Key, D., Lund, J. J., Turbe-Doan, A., Kist, R., Aw, A., Chen, Y., Maas, R. L. and Peters, H.** (2010). Genetic interactions between Pax9 and Msx1 regulate lip development and several stages of tooth morphogenesis. *Dev Biol* **340**, 438-449.

**Niida, A., Hiroko, T., Kasai, M., Furukawa, Y., Nakamura, Y., Suzuki, Y., Sugano, S. and Akiyama, T.** (2004). DKK1, a negative regulator of Wnt signaling, is a target of the beta-catenin/TCF pathway. *Oncogene* **23**, 8520-8526.

**O'Connell, D. J., Ho, J. W., Mammoto, T., Turbe-Doan, A., O'Connell, J. T., Haseley, P. S., Koo, S., Kamiya, N., Ingber, D. E., Park, P. J. and Maas, R. L.** (2012). A Wnt-bmp feedback circuit controls intertissue signaling dynamics in tooth organogenesis. *Sci Signal* **5**, ra4.

**Pauws, E., Hoshino, A., Bentley, L., Prajapati, S., Keller, C., Hammond, P., Martinez-Barbera, J. P., Moore, G. E. and Stanier, P.** (2009). Tbx22null mice have a submucous cleft palate due to reduced palatal bone formation and also display ankyloglossia and choanal atresia phenotypes. *Hum Mol Genet* **18**, 4171-4179.

**Pelletier, J. C., Lundquist, J. T. t., Gilbert, A. M., Alon, N., Bex, F. J., Bhat, B. M., Bursavich, M. G., Coleburn, V. E., Felix, L. A., Green, D. M., Green, P., Hauze, D. B., Kharode, Y. P., Lam, H. S., Lockhead, S. R., Magolda, R. L., Matteo, J. J., Mehlmann, J. F., Milligan, C., Murrills, R. J., Pirrello, J., Selim, S., Sharp, M. C., Unwalla, R. J., Vera, M. D., Wrobel, J. E., Yaworsky, P. and Bodine, P. V.** (2009). (1-(4-(Naphthalen-2-yl)pyrimidin-2-yl)piperidin-4-yl)methanamine: a wingless beta-catenin agonist that increases bone formation rate. *J Med Chem* **52**, 6962-6965.

**Peters, H., Neubuser, A., Kratochwil, K. and Balling, R.** (1998). Pax9-deficient mice lack pharyngeal pouch derivatives and teeth and exhibit craniofacial and limb abnormalities. *Genes Dev* **12**, 2735-2747.

**Recker, R. R., Benson, C. T., Matsumoto, T., Bolognese, M. A., Robins, D. A., Alam, J., Chiang, A. Y., Hu, L., Krege, J. H., Sowa, H., Mitlak, B. H. and Myers, S. L.** (2015). A randomized, double-blind phase 2 clinical trial of blosozumab, a sclerostin antibody, in postmenopausal women with low bone mineral density. *J Bone Miner Res* **30**, 216-224.

**Satokata, I. and Maas, R.** (1994). Msx1 deficient mice exhibit cleft palate and abnormalities of craniofacial and tooth development. *Nat Genet* **6**, 348-356.

**Stapleton, P., Weith, A., Urbanek, P., Kozmik, Z. and Busslinger, M.** (1993). Chromosomal localization of seven PAX genes and cloning of a novel family member, PAX-9. *Nat Genet* **3**, 292-298.

**Stockton, D. W., Das, P., Goldenberg, M., D'Souza, R. N. and Patel, P. I.** (2000). Mutation of PAX9 is associated with oligodontia. *Nat Genet* **24**, 18-19.

**Tan, K., Shaw, A. L., Madsen, B., Jensen, K., Taylor-Papadimitriou, J. and Freemont, P. S.** (2003). Human PLU-1 Has transcriptional repression properties and interacts with the developmental transcription factors BF-1 and PAX9. *J Biol Chem* **278**, 20507-20513.

**van den Boogaard, M. J., Creton, M., Bronkhorst, Y., van der Hout, A., Hennekam, E., Lindhout, D., Cune, M. and Ploos van Amstel, H. K.** (2012). Mutations in WNT10A are present in more than half of isolated hypodontia cases. *J Med Genet* **49**, 327-331.

**Zhang, Y., Zhao, X., Hu, Y., St Amand, T., Zhang, M., Ramamurthy, R., Qiu, M. and Chen, Y.** (1999). Msx1 is required for the induction of Patched by Sonic hedgehog in the mammalian tooth germ. *Dev Dyn* **215**, 45-53.

**Zhang, Z., Song, Y., Zhao, X., Zhang, X., Fermin, C. and Chen, Y.** (2002). Rescue of cleft palate in Msx1-deficient mice by transgenic Bmp4 reveals a network of BMP and Shh signaling in the regulation of mammalian palatogenesis. *Development* **129**, 4135-4146.

**Zhou, J., Gao, Y., Lan, Y., Jia, S. and Jiang, R.** (2013). Pax9 regulates a molecular network involving Bmp4, Fgf10, Shh signaling and the Osr2 transcription factor to control palate morphogenesis. *Development* **140**, 4709-4718.

**Zhou, J., Gao, Y., Zhang, Z., Zhang, Y., Maltby, K. M., Liu, Z., Lan, Y. and Jiang, R.** (2011). Osr2 acts downstream of Pax9 and interacts with both Msx1 and Pax9 to pattern the tooth developmental field. *Dev Biol* **353**, 344-353.

## Figures

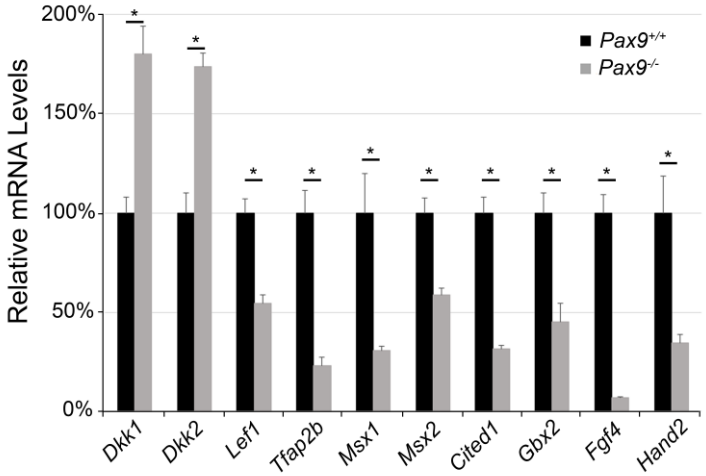


**Fig. 1. Quantitative reverse transcription PCR (RT-PCR) analysis of gene expression in E13.5 *Pax9*$^{-/-}$ palatal shelves.** The mRNA levels of a select group of differentially expressed genes were verified in micro-dissected palatal shelves of *Pax9*$^{+/+}$ and *Pax9*$^{-/-}$ embryos by quantitative RT-PCR (n=5 per group). *Pax9* deficiency affects the expression of Wnt signaling pathway genes and known partner genes of *Pax9*. The expression levels of *Dkk1 and Dkk2* expression are significantly up regulated in the absence of *Pax9*. On the other hand, Wnt signaling pathway downstream targets, such as *Lef1*, *Gbx2*, *Fgf4* and *Hand2*, as well as *Pax9* partner genes *Msx1* and *Msx2* were significantly down regulated in *Pax9*$^{-/-}$ samples. Results are shown as percentage of the mean of *Pax9*$^{+/+}$ group ± s.e.m. Error bars indicate s.e.m., * $P < 0.01$.

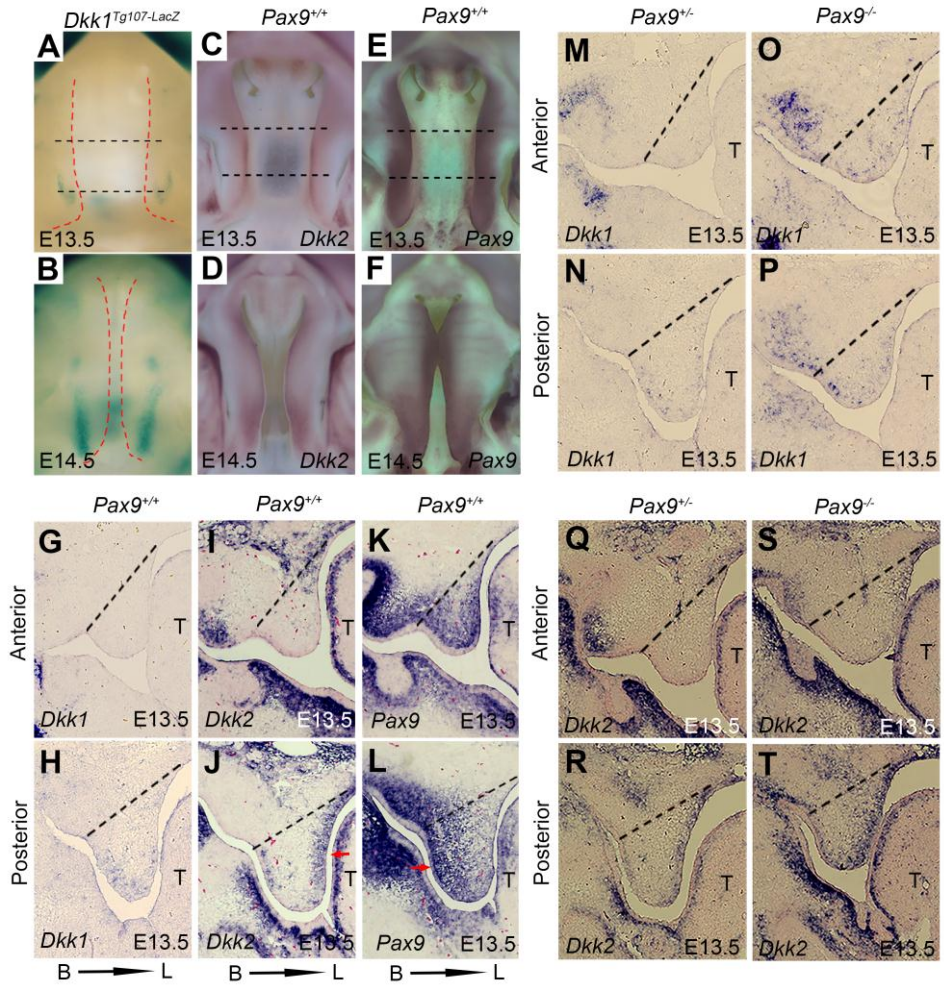


**Fig. 2. Patterns of *Pax9*, *Dkk1* and *Dkk2* expression in E13.5 *Pax9*$^{+/-}$ and *Pax9*$^{-/-}$ palatal shelves suggest that Pax9 is upstream of Wnt signaling.**

(A, B) Whole mount LacZ staining showed that *Dkk1* expression appears restricted to the posterior domain of palatal in *Dkk1*$^{Tg107\text{-}LacZ}$ embryos at E13.5 and E14.5, respectively. Red dashed lines indicate the boundary of palate. (C, D) whole mount *in-situ* hybridization showed that *Dkk2* transcripts (purple) are more visible at the medial edges of the palatal shelves on *Pax9*$^{+/+}$ embryos at E13.5 (C) and E14.5 (D). (E, F) In contrast, *Pax9* expression appears stronger and expands along the anterior-posterior domain of palatal shelves at E13.5 and E14.5, respectively. Black dashed lines indicate the position of the sections in panels (G-N). Panels (A) and (B) represent beta-galactosidase staining in palatal tissues where Dkk1 is expressed while panels (C-F)

are colored differently as they compare endogenous *Dkk2* and *Pax9* mRNA transcripts detected after whole-mount hybridization of digoxygenin-labeled probes.

(G-L) Results of sectional in situ hybridizations using adjacent sections, presented in the coronal plane, confirm that *Dkk1* and *Dkk2* transcripts have inverse expression patterns with that of *Pax9* at E13.5 and E14.5. While *Pax9* expression is more intense along the buccal aspects of palatal mesenchyme (K, L), *Dkk2* transcripts localize on the lingual side (I-L) consistent with our observations. (M-P) In the posterior regions of palatal mesenchyme, *Dkk1* and *Dkk2* expression increased at E13.5 as a result of *Pax9* deficiency. B, buccal; L, lingual; T, tongue; dashed lines indicate the boundary of palate, red arrows indicate the higher expression domain. n=6 for whole mount *in-situ* hybridization, n=5 for sectioned *in-situ* hybridizations.

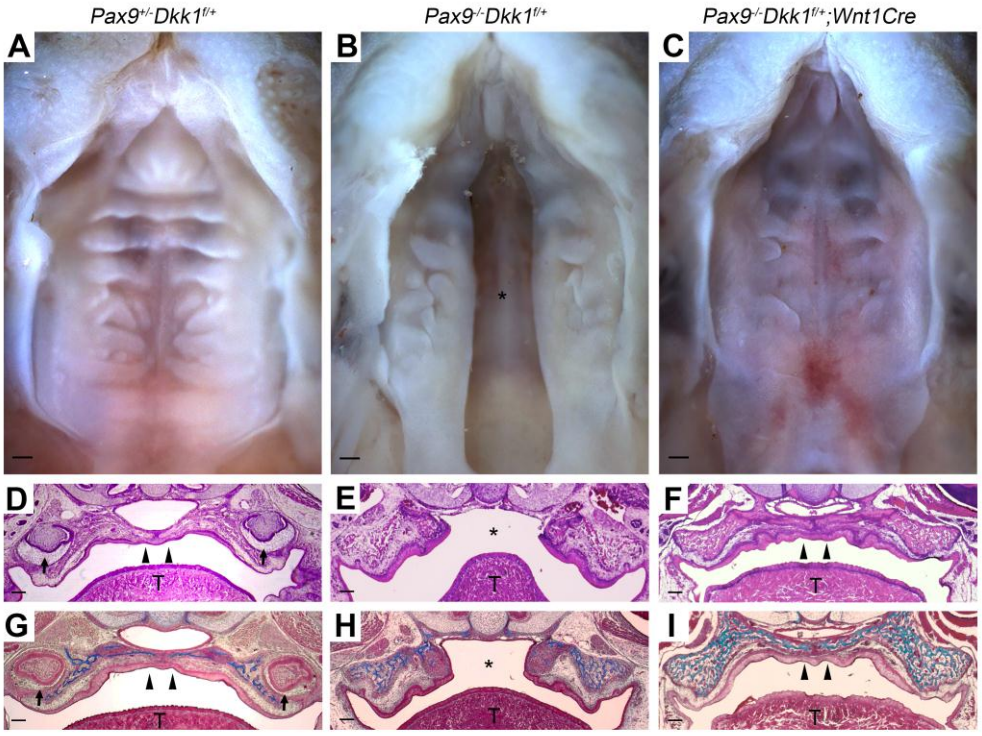


**Fig. 3. Genetic reduction of *Dkk1* expression rescued secondary palate clefts in *Pax9*$^{-/-}$ mice.** Representative whole mount oral views of palate formation in E18.5 *Pax9*$^{+/-}$*Dkk1*$^{f/+}$ (A, D, G), *Pax9*$^{-/-}$*Dkk1*$^{f/+}$ (B, E, H) and *Pax9*$^{-/-}$*Dkk1*$^{f/+}$*;Wnt1Cre* (C, F, I) embryos. (A) Palate closure in *Pax9*$^{+/-}$*Dkk1*$^{f/+}$ embryos. (B) The phenotype of cleft palate in *Pax9*$^{-/-}$*Dkk1*$^{f/+}$ embryos (n=4). (C) Intact palate with disordered rugae in *Pax9*$^{-/-}$ *Dkk1*$^{f/+}$*;Wnt1Cre* embryos (n=5). (D-F) H & E staining of coronal sections. (D) Fusion of the palatal shelves in *Pax9*$^{+/-}$*Dkk1*$^{f/+}$ embryo. (E) Failure of palatal shelf outgrowth and closure in a *Pax9*$^{-/-}$*Dkk1*$^{f/+}$ embryo. (F) The cleft defect is reversed genetically in a *Pax9*$^{-/-}$*Dkk1*$^{f/+}$*;Wnt1Cre* embryo. (G-I) Masson's Trichrome staining of serial sections show the deposition of connective tissue (blue color) within the palatal shelves (G) *Pax9*$^{+/-}$*Dkk1*$^{f/+}$ and (I) *Pax9*$^{-/-}$*Dkk1*$^{f/+}$*;Wnt1Cre* embryos, while only maxillary bone tissue was stained blue in *Pax9*$^{-/-}$*Dkk1*$^{f/+}$ (H). T, tongue; * indicates cleft palate; black arrowheads indicate intact palate shelve; black arrows indicate molars. Scale bars indicate 200 μm.

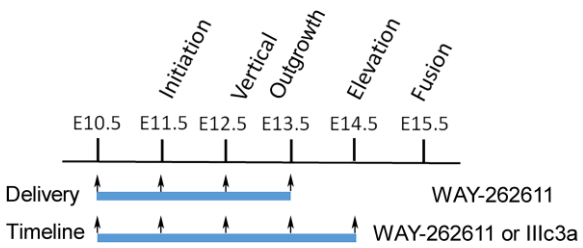


**Fig. 4. Controlled delivery schedule for small-molecule Wnt agonists.** WAY-262611 or IIIc3a was intravenously injected through tail vein during the designed periods (blue bars). WAY-262611 was injected for 2 timelines E10.5 - E13.5 and E10.5 - E14.5; the timeline for delivery of IIIc3a injection was E10.5 - E14.5 based on the high rate of palatal closure achieved with WAY-262611 (see Table 2 for details). Black arrows indicate daily injection.

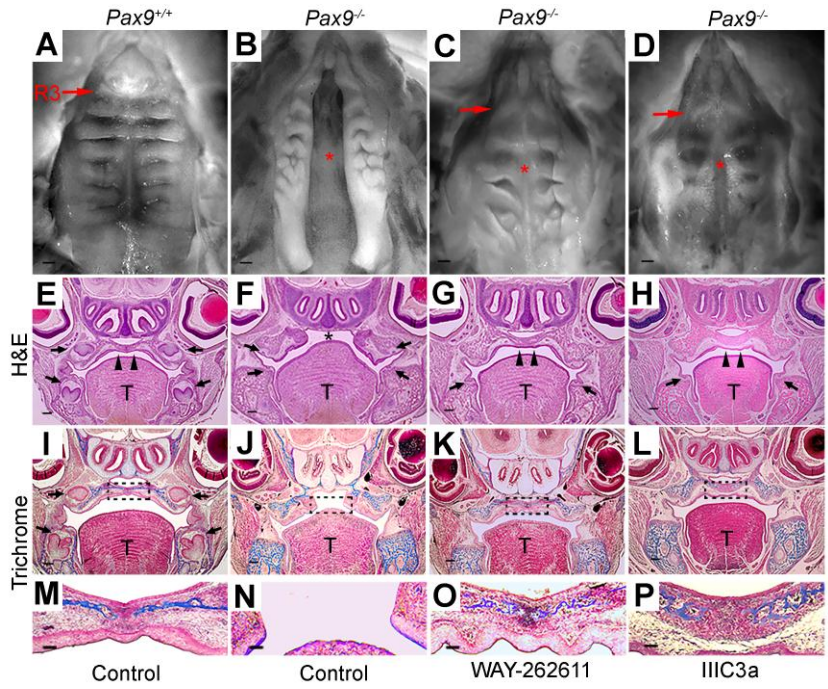


**Fig. 5. Fusion of the secondary palate in *Pax9*$^{-/-}$ embryos after intravenous delivery of small-molecule Wnt agonists.** (A-D) Representative whole mount oral views of palatal shelves. (A) In a *Pax9*$^{+/+}$ embryo at E18.5, normal palatal fusion with parallel rugae arrangement is visible. (B) Cleft in the secondary palate was a consistent phenotype in control treated *Pax9*$^{-/-}$ embryos at E18.5 (n=10). (C, D) Intravenous delivery of WAY-262611 (n=18) and III3ca (n=12) led to the closure of palatal shelves in the midline (red asterisk). However, rugae appear less organized when compared to *Pax9*$^{+/+}$ embryos. R3, Ruga 3; red arrows indicate the 3$^{rd}$ ruga; red asterisk indicates cleft palate or secondary palate fusion after treatment. (E-H) Hematoxylin and Eosin (H&E) staining of coronal sections through E18.5 heads, showed that the palatal shelves were fused in *Pax9*$^{+/+}$ mice (E) while a cleft palate was visible in a mutant littermate (F). Note the arrest in tooth formation at the bud stage (black arrows). As compared to controls that received control injections (F), closure of the palatal shelves was clearly evident in WAY-262611 and IIIc3a treated *Pax9*$^{-/-}$ mice (G, H, respectively). Note that in treated mice, tooth organs did not advance beyond the early cap stage (black arrows). (I-P) Masson's Trichrome staining of position-matched sections showed that the deposition of connective tissue (blue color) within the palatal shelves of WAY-

262611 (K,O) and IIIc3a treated (L,P) *Pax9*$^{-/-}$ mice resembled that visible in control samples (I,J,M,N). T, tongue; arrowheads indicate intact palate shelves; balck arrows indicate the first molar; dashed rectangle in (I-L) represents the enlarged area of (M-P).

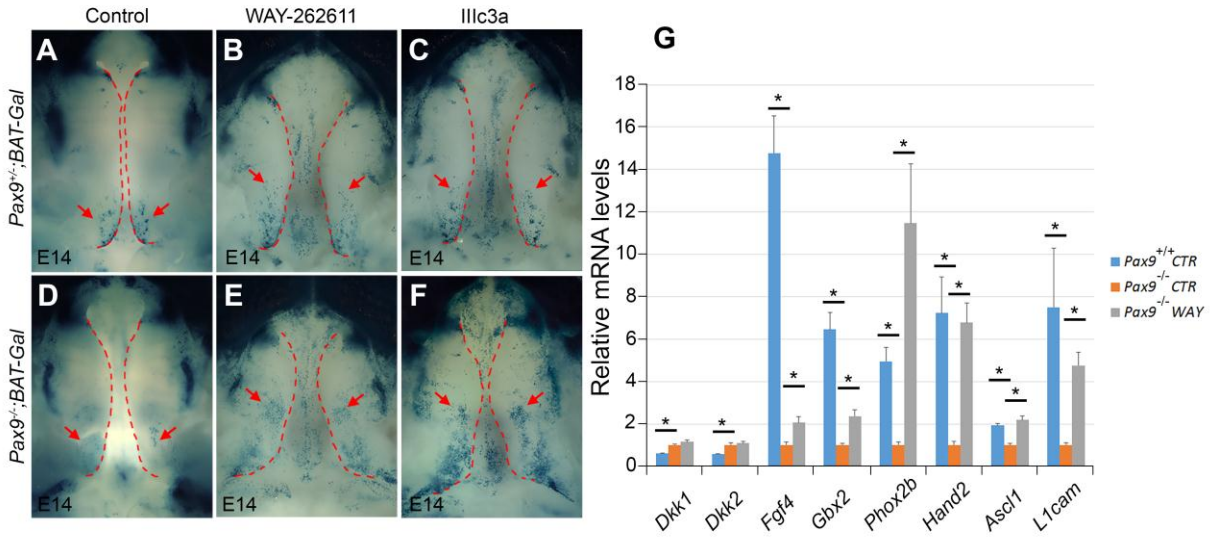


**Fig. 6. Wnt signaling activity and the expression of downstream targets were partially restored in *Pax9*$^{-/-}$ palate after treatments. (A-F)** Whole mount LacZ staining (blue color) of *Pax9*$^{-/-}$*; BAT-Gal* mice at E14.0 to assess Wnt signaling activity after Wnt agonist therapies. WAY-262611 and IIIc3a slightly increased Wnt activity in the posterior palatal region of *Pax9*$^{+/-}$*; BAT-Gal* mice (compare A to B, C). However, a more significant and expanded level of Wnt activity is observed within posterior palatal shelves of *Pax9*$^{-/-}$*; BAT-Gal* mice (Compare D to E, F). Red arrows point to the Wnt signaling activity in palate; dashed line indicates the boundary of palate. (**G**) The mRNA levels of selected differentially expressed genes were verified by quantitative RT-PCR using E13.5 micro-dissected palatal shelves (n=5). Error bars indicate s.e.m., * $P < 0.01$.

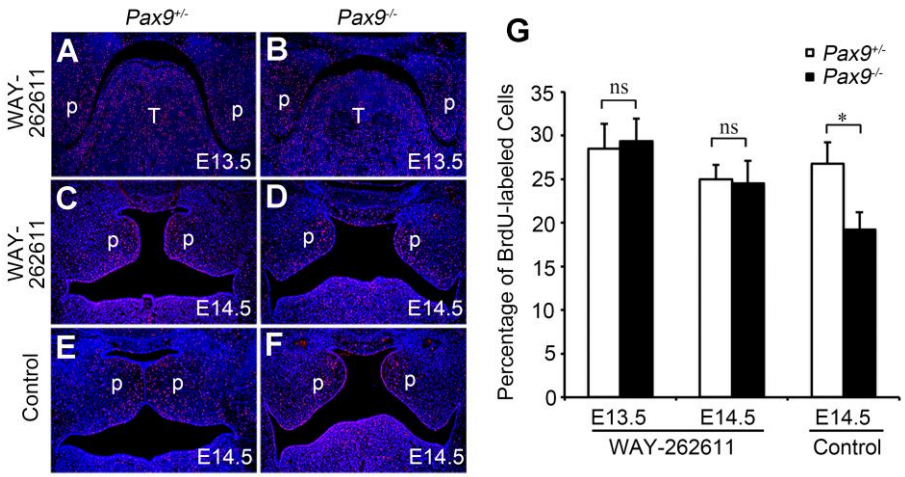


**Fig. 7. Cell proliferation in the palate of WAY-262611 treated *Pax9*$^{-/-}$ mice.** Representative images of sections through the posterior regions of the palate in E13.5 (A, B), E14.5 *Pax9*$^{+/-}$ (C, E) and *Pax9*$^{-/-}$ (D, F) embryos with (A-D) or without WAY-262611 treatment (E, F). Red signals showed the distribution of BrdU-labeled nuclei. Blue signals showed the total nuclei, which were stained with Hoechst. T, tongue; p, palate shelf. (G) The percentage of BrdU-labeled cells in the palatal mesenchyme. n=5, error bar represents s.d. *, $P < 0.01$. ns, no significance.

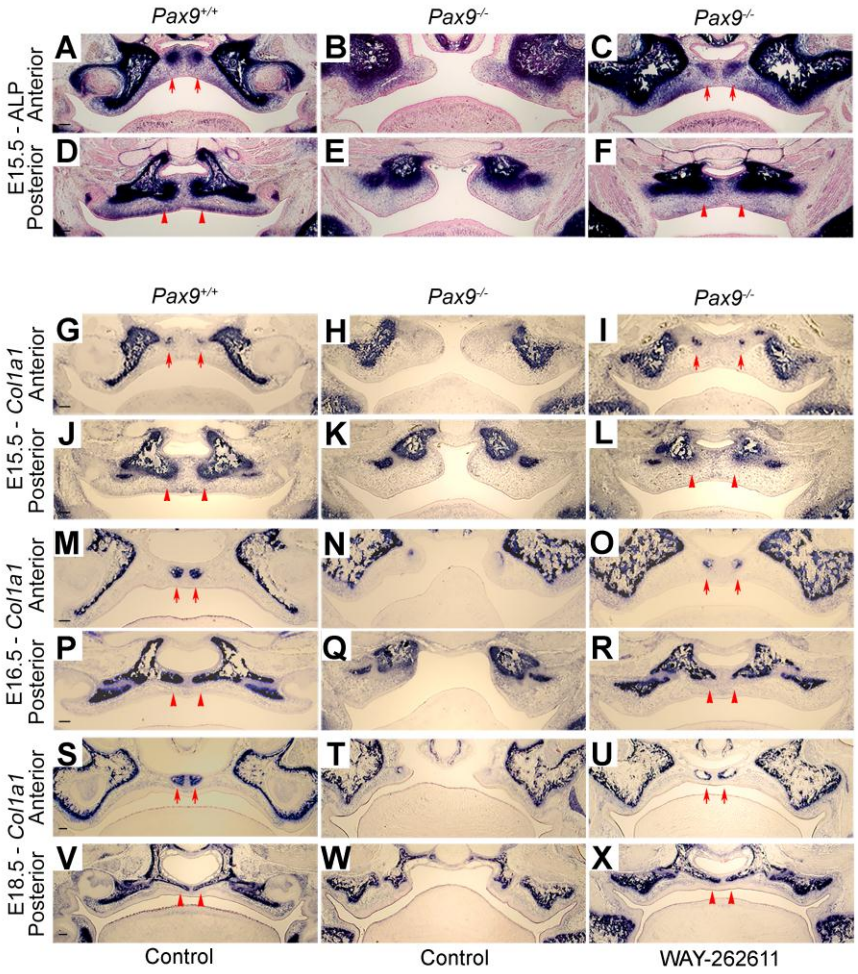


**Fig. 8. The restoration of osteogenesis in WAY-262611 treated *Pax9*$^{-/-}$ palatal shelves.** (A-F) Detection of alkaline phosphatase activity in the palatal mesenchyme during palatal bone formation in *Pax9*$^{+/+}$ and *Pax9*$^{-/-}$ embryos without or with WAY-262611 treatment. Position-matched coronal sections of E15.5 embryos through the anterior and posterior palates are used. (A, D) Alkaline phosphatase activity (blue coloration) was detected in the palate of *Pax9*$^{+/+}$ embryos but not in *Pax9*$^{-/-}$ embryos (B, E). After Wnt agonist treatment, enzymatic activity was detected in the *Pax9*$^{-/-}$ palate (C, F). Red arrows point to osteogenic centers of the developing palatal processes of the maxilla. Red arrowheads, prospective palatal processes of the palatine bone. (G-X) Comparison of expression of *Col1a1* mRNA in the palatal mesenchyme during palatal bone formation in *Pax9*$^{+/+}$ and *Pax9*$^{-/-}$ embryos without or with WAY-262611 treatment. Position-matched coronal sections of E15.5 (G-L), E16.5 (M-R) and E18.5 (S-X)

embryos through the anterior and posterior palates are used. Expression of *Col1a1* was detected within osteogenic zones as early as E15.5 (G, J) and increased from E16.5 (M, P) to E18.5 (S, V) in *Pax9*$^{+/+}$ palates. In *Pax9*$^{-/-}$ palate, expression of *Col1a1* was highly reduced (H, K, N, Q, T and W). After Wnt agonist treatment, *Col1a1* expression was restored in the palate of *Pax9*$^{-/-}$ embryos (I, L, O, R, U and X). mRNA signals are shown in blue color. Red arrows, osteogenic centers of the developing palatal processes of the maxilla. Red arrowheads, prospective palatal processes of the palatine bone. n=5 for each assay.

## Tables

Table 1. Expression profiles of *Pax9* affected genes with functional enrichment analysis in E13.5 palatal shelves

| Gene | *Pax9*$^{+/-}$ | *Pax9*$^{-/-}$ | FC | *P*-value | Gene | *Pax9*$^{+/-}$ | *Pax9*$^{-/-}$ | FC | *P*-value |
|---|---|---|---|---|---|---|---|---|---|
| ***Dkk1*** | 180.64 | 324.53 | 1.80 | 3.88E-03 | ***Tfap2b*** | 2405.06 | 873.21 | -2.75 | 3.22E-85 |
| ***Dkk2*** | 3199.37 | 4888.36 | 1.52 | 8.71E-13 | ***Msx1*** | 6554.76 | 3221.79 | -2.03 | 2.22E-41 |
| ***Wnt7a*** | 25.82 | 6.91 | -3.74 | 0.005 | ***Msx2*** | 477.41 | 265.37 | -1.80 | 4.58E-04 |
| ***Wnt3*** | 42.53 | 20.30 | -2.09 | 5.58E-03 | ***Bmp4*** | 1522.38 | 867.67 | -1.75 | 2.82E-16 |
| ***Wnt9b*** | 65.42 | 35.74 | -1.83 | 3.34E-03 | ***Osr2**** | 6338.19 | 11254.15 | -1.72 | 7.98E-24 |
| ***Lef1*** | 1231.91 | 600.32 | -2.05 | 1.02E-16 | ***Foxf1*** | 5657.10 | 3784.74 | -1.50 | 3.81E-10 |
| ***Rspo1*** | 982.53 | 631.61 | -1.56 | 8.00E-03 | ***Hand2*** | 165.14 | 63.62 | -2.59 | 1.06E-10 |
| ***Gbx2*** | 26.34 | 6.24 | -4.22 | 4.29E-05 | ***Cited1*** | 404.22 | 165.68 | -2.44 | 1.28E-07 |
| ***Gad1*** | 32.42 | 4.53 | -7.16 | 6.87E-14 | ***Ret*** | 550.22 | 149.65 | -3.68 | 1.99E-22 |
| ***Fgf4*** | 109.69 | 9.22 | -11.90 | 2.93E-05 | ***Hoxa2*** | 28.37 | 2.77 | -10.24 | 3.39E-03 |
| ***Edar*** | 184.38 | 98.87 | -1.86 | 3.41E-05 | ***Ryr1*** | 876.49 | 2062.90 | 2.35 | 7.30E-03 |

The expression levels were shown by normalized counts. FC, Fold Change; -, down-regulation. *, normalized counts using reads from endogenous *Osr2*.

Table 2. Secondary palate closure after treatments with Wnt agonists.

| Drugs | Expt. Groups | Time Line | Dosage (mg/Kg) | *Pax9*$^{-/-}$ No. | Closure | Cleft Palate |
|---|---|---|---|---|---|---|
| WAY-262611 | 1 | E10.5-14.5 | 12.5 | 6 | 6/2* | 0 |
| | 2 | E10.5-14.5 | 25 | 12 | 12/5* | 0 |
| | 3 | E10.5-13.5 | 12.5 | 8 | 3/1* | 5 |
| | 4 | E10.5-13.5 | 25 | 9 | 6/3* | 3 |
| IIIc3a | 5 | E10.5-14.5 | 12.5 | 9 | 7/3* | 2 |
| | 6 | E10.5-14.5 | 25 | 6 | 5/3* | 1 |

*, number of *Pax9*$^{-/-}$ embryos with small residual fusion defects between the primary and secondary palates.

Table 3. Differentially Expressed Genes in *Pax9*$^{-/-}$ Samples with or without Treatment

| | *Pax9*$^{-/-}$ WAY | *Pax9*$^{+/+}$ WAY | *Pax9*$^{-/-}$ CTR | *Pax9*$^{+/+}$ CTR | FC-CTR mut/WT | FC-*Pax9*$^{-/-}$ WAY/CTR |
|---|---|---|---|---|---|---|
| *Fgf4* | 11.91 | 73.41 | 4.96 | 152.77 | -30.77* | 2.40* |
| *Gbx2* | 9.95 | 22.39 | 4.15 | 27.50 | -6.62* | 2.40* |
| *Hoxb2* | 4.50 | 17.99 | 1.28 | 8.15 | -6.36* | 3.51* |
| *Phox2b* | 310.88 | 366.25 | 40.25 | 193.65 | -4.81* | 7.72* |
| *Phox2a* | 157.04 | 203.49 | 22.93 | 86.78 | -3.78* | 6.85* |
| *Hand2* | 177.22 | 219.69 | 36.10 | 127.48 | -3.53* | 4.91* |
| *Mmp7* | 6.88 | 4.59 | 2.22 | 5.85 | -2.64* | 3.10* |
| *Ascl1* | 109.57 | 121.37 | 38.55 | 92.15 | -2.39* | 2.84* |
| *Hmx3* | 22.26 | 29.60 | 9.06 | 16.56 | -1.83* | 2.46* |
| *Alk* | 120.52 | 128.84 | 70.67 | 114.27 | -1.62* | 1.71* |
| *L1cam* | 981.37 | 1276.89 | 634.81 | 919.99 | -1.45 | 1.55* |
| *Mmp24* | 50.47 | 47.89 | 24.82 | 31.41 | -1.27 | 2.03* |
| *Gfi1* | 14.63 | 11.42 | 9.02 | 9.67 | 0.93 | 1.62* |
| *Tnnt3* | 678.95 | 489.04 | 431.67 | 439.72 | 0.98 | 1.57* |
| *Ush1c* | 5.31 | 9.96 | 8.50 | 8.09 | 1.05 | -1.60* |
| *Otop1* | 3.68 | 2.00 | 10.54 | 9.97 | 1.06 | -2.87* |
| *Ccl2* | 38.07 | 73.20 | 69.29 | 64.58 | 1.07 | -1.82* |
| *Tmc1* | 6.88 | 4.90 | 11.82 | 6.11 | 1.93* | -1.72* |
| *Slc17a8* | 13.17 | 14.30 | 29.78 | 13.21 | 2.25* | -2.26* |

The expression levels were shown by normalized counts. FC, Fold Change; -, down-regulation; *, $P < 0.01$; WAY, WAY-262611 treatments; CTR, control treatments;

## Supplementary Figures

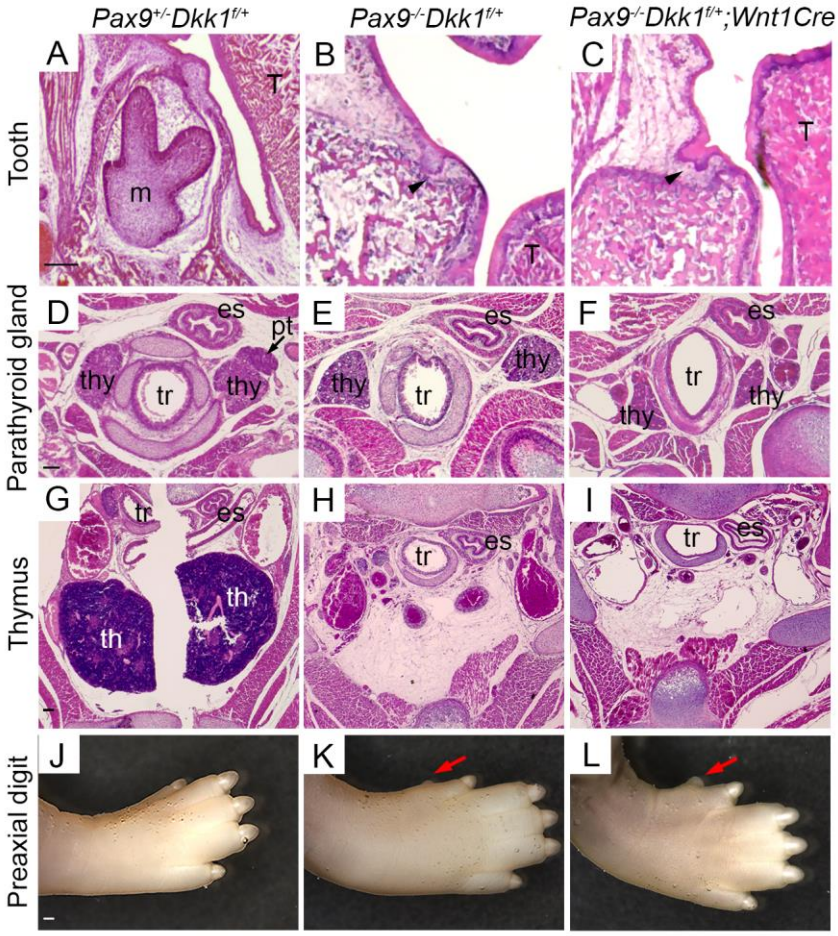


**Figure S1. Reducing *Dkk1* in compound mutants of *Pax9*$^{-/-}$*Dkk1*$^{f/+}$*;Wnt1Cre* failed to rescue the defects of tooth organs, parathyroid glands, thymus and hind limb in *Pax9*$^{-/-}$ embryos.** (A-C) H&E staining of sections through developing 1$^{st}$ molar in P0 pups. Compared with late bell stage in *Pax9*$^{+/-}$*Dkk1*$^{f/+}$ (A), tooth development arrested at bud stage in *Pax9*$^{-/-}$*Dkk1*$^{f/+}$ (B, black arrowhead) while the 1$^{st}$ molar advanced to early cap stage in *Pax9*$^{-/-}$*Dkk1*$^{f/+}$*;Wnt1Cre* (C, black arrowhead). (D-F) H&E staining of sections through thyroid in P0 embryos. Parathyroid gland is near the dorsolateral border of the thyroid lobe in *Pax9*$^{+/-}$*Dkk1*$^{f/+}$ samples (D, black arrow) but missing in *Pax9*$^{-/-}$*Dkk1*$^{f/+}$ (E) and *Pax9*$^{-/-}$*Dkk1*$^{f/+}$*;Wnt1Cre* embryos (F). (G-I) H&E staining of sections through thymus position in P0 embryos. Compared with the dark-stained thymus in *Pax9*$^{+/-}$*Dkk1*$^{f/+}$ samples (G), *Pax9*$^{-/-}$*Dkk1*$^{f/+}$ (H) and *Pax9*$^{-/-}$*Dkk1*$^{f/+}$*;Wnt1Cre* embryos (I) showed lack of thymus. (J-L) The ventral views of hind limb. In comparison

to the normal digits in *Pax9*$^{+/-}$*Dkk1*$^{f/-}$ samples (J), *Pax9*$^{-/-}$*Dkk1*$^{f/+}$ (K) and *Pax9*$^{-/-}$*Dkk1*$^{f/+}$*;Wnt1Cre* embryos (L) had extra-formed digit (red arrows in K and L). es, esophagus; m, molar; pt, parathyroid gland; T, tongue; th, thymus; thy, thyroid; tr, trachea. Scale bar represents 100µm.

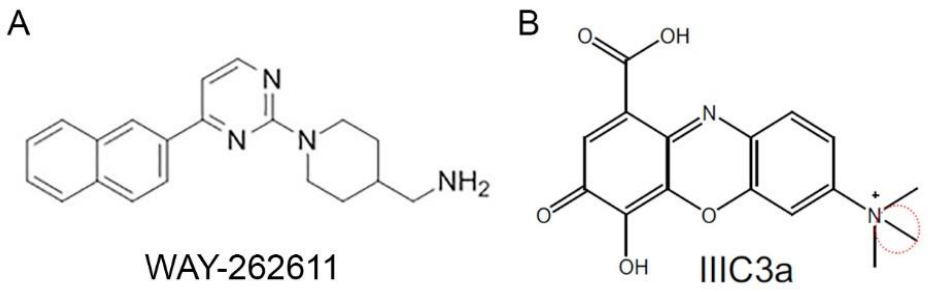


**Figure S2. The structure formula of Wnt agonists used for treatments.** (A) Dkk1 inhibitor, WAY-262611; (B) Dkk inhibitor II, IIIc3a (Pelletier et al., 2009; Li et al., 2012).

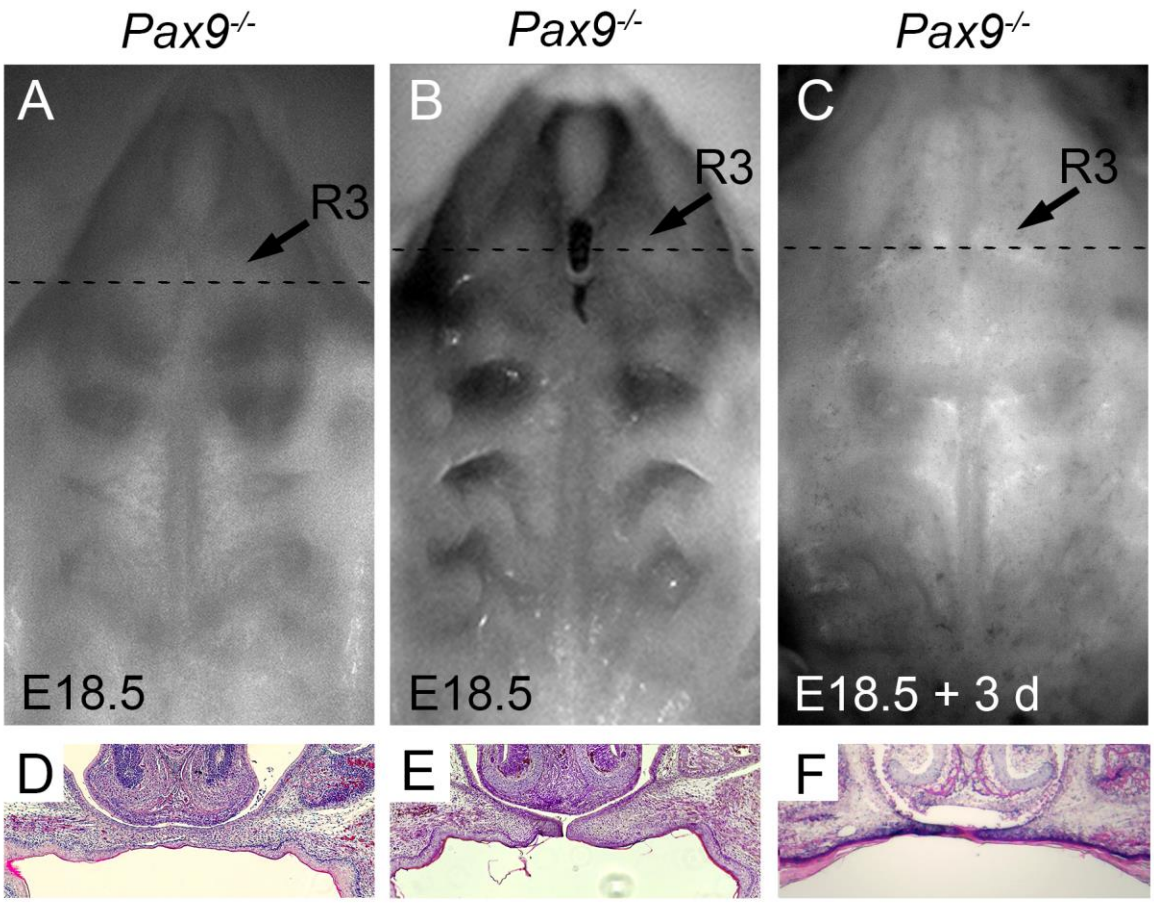


**Figure S3. The residual fusion defects in the treated *Pax9*$^{-/-}$ samples were rescued after 3 days of culture.** The whole mount view of palates treated with WAY-262611 *in-utero* (A, B) and with additional 3 days of culture after WAY-262611 *in-utero* treatment (C). 60% (11 in 18) *Pax9*$^{-/-}$ embryos showed full closure of palate shelves (A) and 40% (7 in 18) *Pax9*$^{-/-}$ embryos showed residual fusion defects between primary and secondary palate (B). The residual fusion defects were resolved *in-vitro* after culture for 3 days (n=5) (C). Dashed line indicates the position of section in D, E, F, respectively. Black arrows point the position of the 3$^{rd}$ ruga (R3). HE staining of frontal sections through palates showed fully closure (D), small gap at the 3$^{rd}$ ruga (E) and the gap disappeared after 3 days of culture (F).

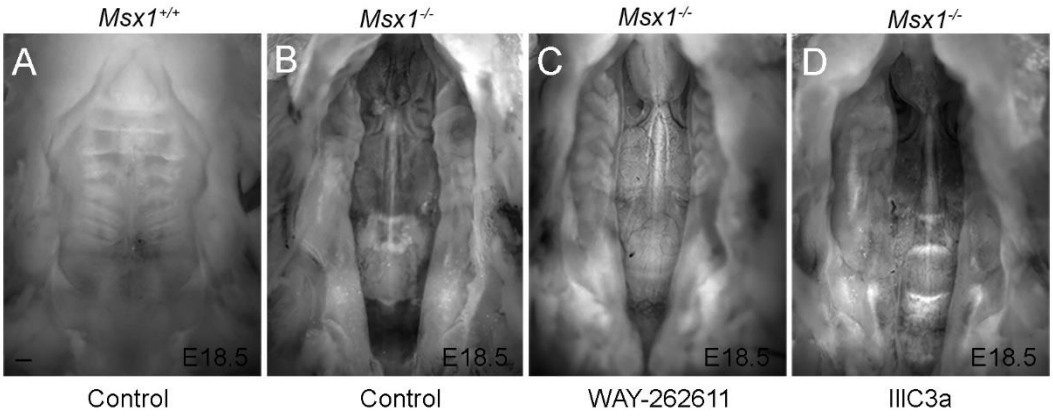


**Figure S4. The treatments with Wnt signaling agonists didn't rescue cleft palate in *Msx1*$^{-/-}$ embryos.** Compared with intact palate in *Msx1*$^{+/+}$ embryo (A), all the *Msx1*$^{-/-}$ embryo (B), WAY-262611 treated *Msx1*$^{-/-}$ embryos (C, 15 samples) and IIIc3a treated *Msx1*$^{-/-}$ embryos (D, 34 samples) showed 100% penetrance of the complete cleft palate.

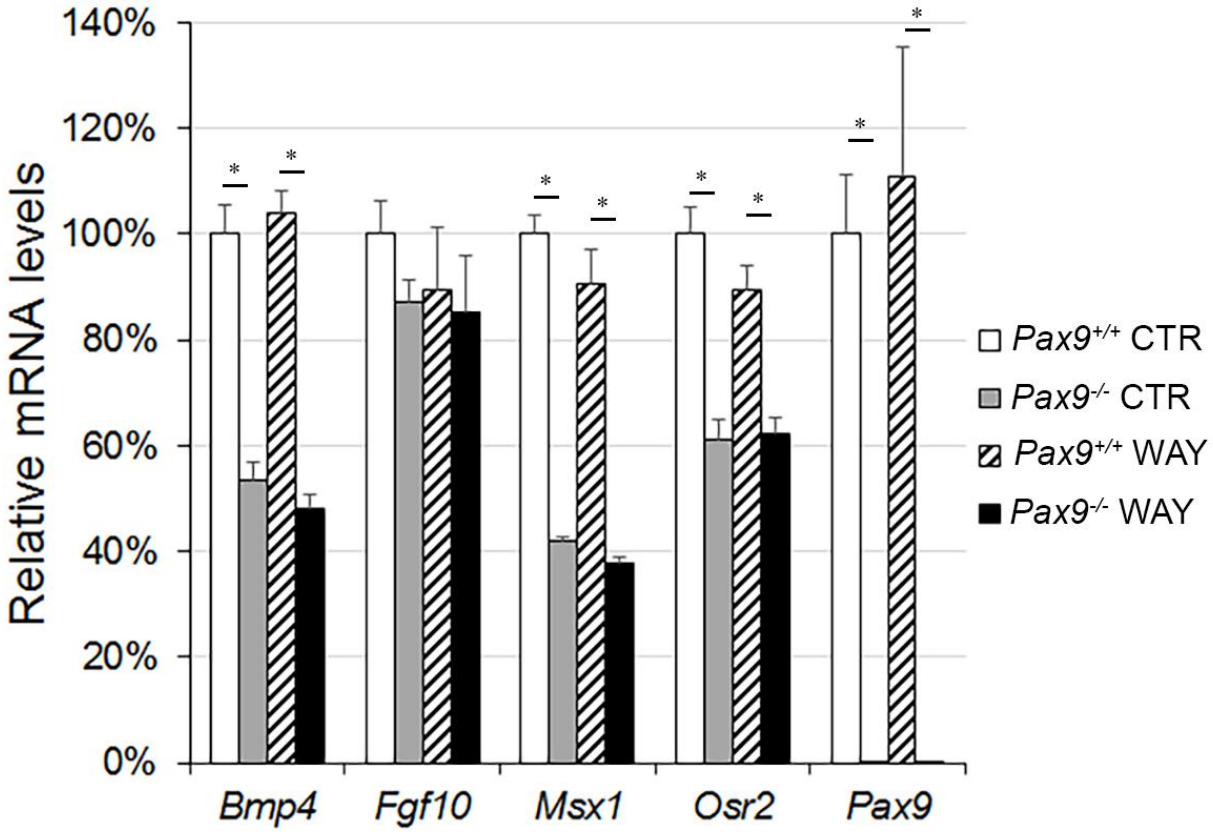


**Figure S5. Quantitative RT-PCR analysis of gene expression of known Pax9 targets from control and WAY-262611 treated groups.** In *Pax9*$^{-/-}$ samples, the expression levels of endogenous *Osr2, Msx1* and *Bmp4* were significantly reduced while *Fgf10* mRNA was moderately decreased. Treatment with Wnt signaling agonist WAY-262611 did not appear to restore levels of *Bmp4, Msx1, Fgf10* and *Osr2* expression. Error bars indicate s.e.m., * $P < 0.05$. CTR, control treatment; WAY, WAY-262611 treatment.

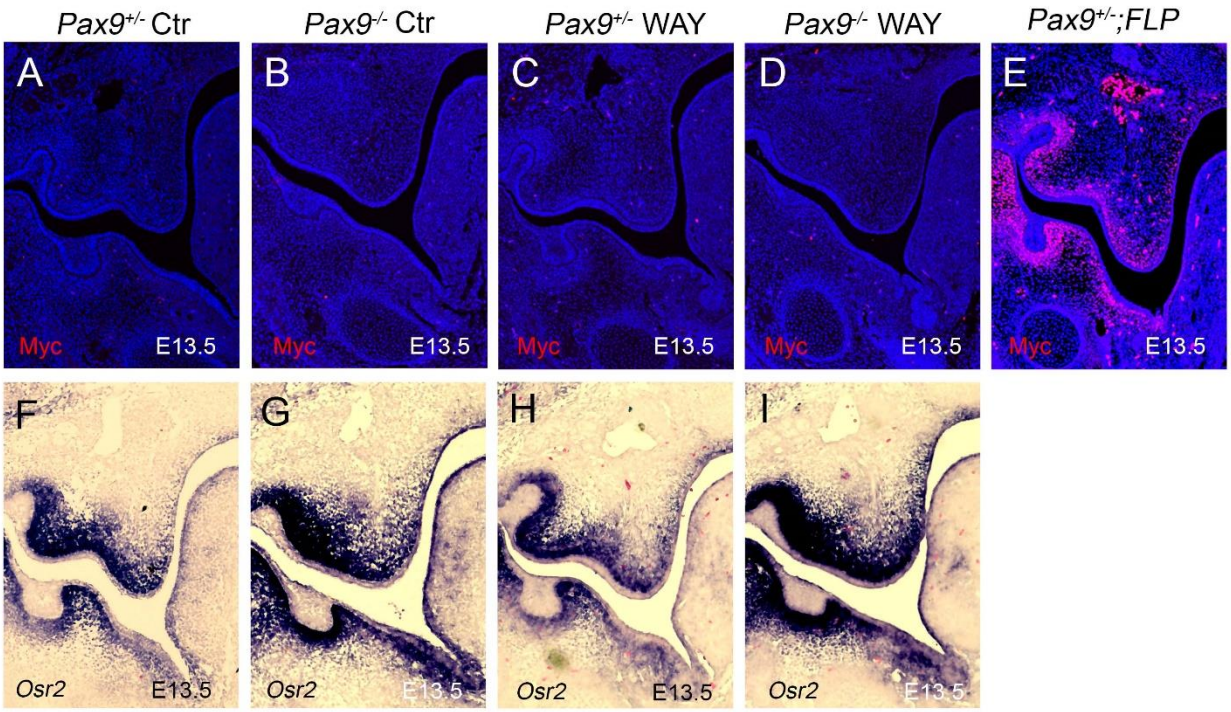


**Figure S6. The knock-in *Myc-Osr2* was not translated into protein in the palate after WAY-262611 treatment.** (A-E) Lack of detection of Myc-Osr2 protein in E13.5 palate frontal sections in WAY-262611 treated embryos using anti-Myc antibody. No Myc-staining was detected in *Pax9*$^{+/-}$ or *Pax9*$^{-/-}$ samples with control or WAY-262611 treatment (A-D). *Pax9*$^{+/-}$*;FLP* (also named *Pax9*$^{Osr2KI}$ in Zhou et al., 2011) sample was used as the positive control to show the strong and specific Myc-staining, in which samples *Myc-Osr2* was translated into protein (E). (F-I) *In-situ* hybridization in E13.5 palate frontal sections using *Osr2*-specific probe. Though stronger *Osr2* signals were detected in *Pax9*$^{-/-}$ samples (G, I) than *Pax9*$^{+/-}$ samples (F, H), representing the transcription of extra copy of transgenic *Osr2*, there is no significant increase of Osr2 expression after WAY-262611 treatment (comparing H with F, I with G). Anti-Myc antibody staining in red and *in-situ* hybridization signals are shown in blue. Ctr, control treatment; WAY, WAY-262611 treatment.

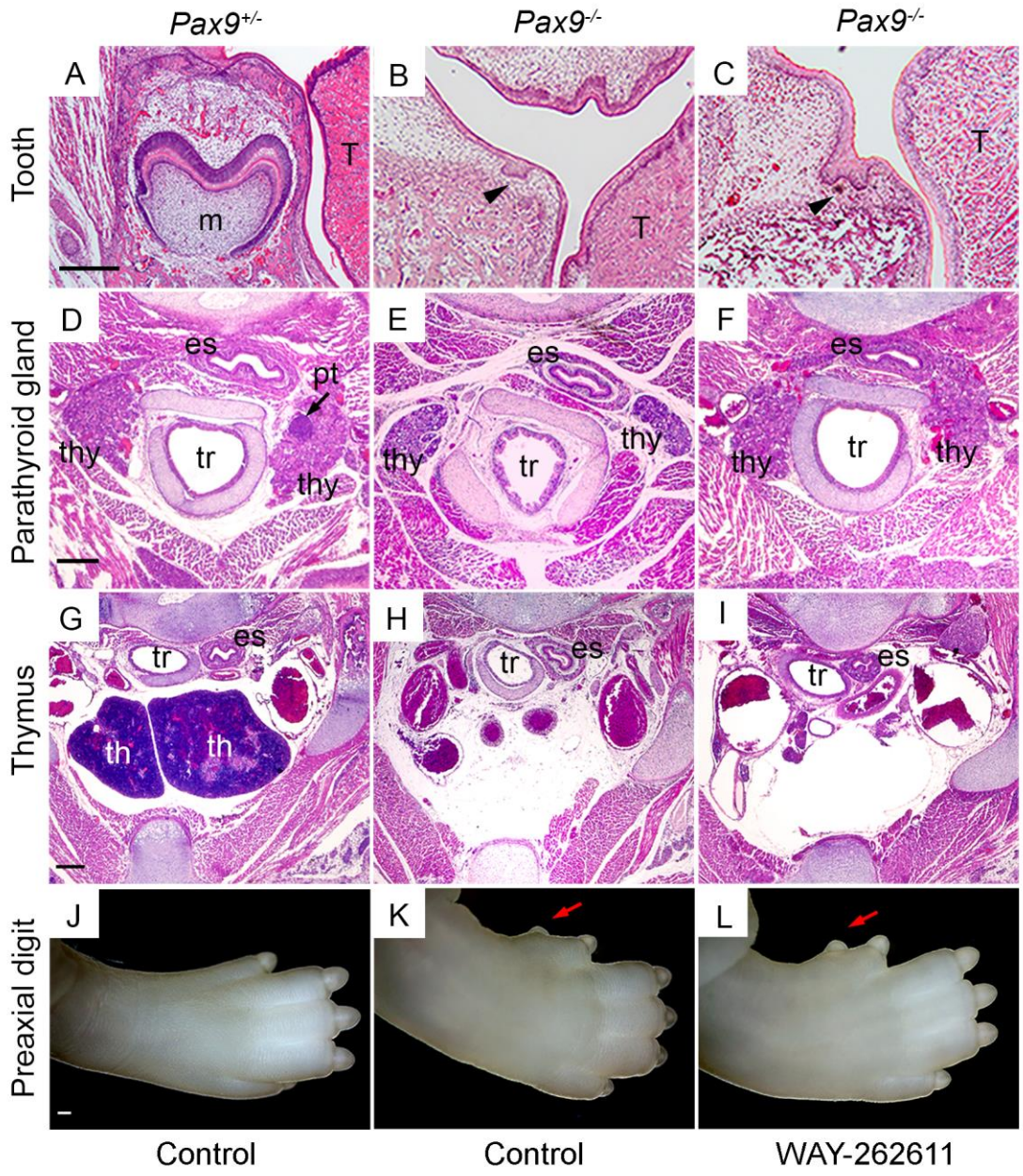


**Figure S7. Wnt agonist therapies failed to rescue the defects of tooth organs, parathyroid glands, thymus, and hind limb in *Pax9*$^{-/-}$ embryos.** (A-C) H&E staining of sections through developing 1$^{st}$ molar at E18.5. Compared with late bell stage in *Pax9*$^{+/-}$ (A), tooth development arrested at bud stage in *Pax9*$^{-/-}$ (B, black arrowhead) while the 1$^{st}$ molar advanced to early cap stage in WAY-262611 treated *Pax9*$^{-/-}$ (C, black arrowhead). (D-F) H&E staining of sections through thyroid of E18.5 embryos. Parathyroid gland is near the dorsolateral border of the thyroid lobe in *Pax9*$^{+/-}$ samples (D, black arrow) but missing in *Pax9*$^{-/-}$ embryos without (E) or with (F) WAY-262611

treatment. (G-I) H&E staining of sections through thymus position in E18.5 embryos. Compared with the dark-stained thymus in *Pax9*$^{+/-}$ samples (G), *Pax9*$^{-/-}$ embryos without (H) or with (I) WAY-262611 treatment showed lack of thymus. (J-L) The ventral views of hind limb. In comparison to the normal digits in *Pax9*$^{+/-}$ samples (J), *Pax9*$^{-/-}$ embryos without (K) or with (L) WAY-262611 treatment had extra-formed digit (red arrows in K and L). es, esophagus; m, molar; pt, parathyroid gland; T, tongue; th, thymus; thy, thyroid; tr, trachea. Scale bar represents 200μm.

**Supplementary Table 1:**
Primers for Quantitative RT-PCR

| Name | Sequence | Name | Sequence |
|---|---|---|---|
| *Bmp4-QF* | GAGGGATCTTTACCGGCTCC | *Cited1-QF* | TCGCTTCGTCCGTACCTCAG |
| *Bmp4-QR* | GTTGAAGAGGAAACGAAAAGCAG | *Cited1-QR* | CTCCTGGTTGGCATCCTCCTT |
| *Dkk1-QF* | AACTACCAGCCCTACCCTTG | *Gbx2-QF* | GCAACTTCGACAAAGCCGAG |
| *Dkk1-QR* | TCTGGGATATCCATCCCCCG | *Gbx2-QR* | GACAGCCCCGACGAGC |
| *Dkk2-QF* | TACTCTTCCAAAGCCAGACTCCA | *Fgf4-QF* | AAGCTCTTCGGTGTGCCTTT |
| *Dkk2-QR* | CCTCATTCTTCCGCATTCCA | *Fgf4-QR* | CGGAGGGTCACAGTCTAGGA |
| *Lef1-QF* | GAAATCATCCCAGCCAGCAA | *Phox2b-QF* | GTACGCCGCAGTTCCATACA |
| *Lef1-QR* | GGGCATCATTATGTAGCCAGAGTA | *Phox2b-QR* | CTGCTTGCGAAACTTAGCCC |
| *Tfap2b-QF* | TACAGACAGCGGAGTCCTGA | *Hand2-QF* | CACCAGCTACATCGCCTACC |
| *Tfap2b-QR* | CATCGTGCCGGTCCTCATAG | *Hand2-QR* | TCTCATTCAGCTCTTTCTTCCTCT |
| *Msx1-QF* | CGGCCATTTCTCAGTCGG | *Ascl1-QF* | TCTCGTCCTACTCCTCCGAC |
| *Msx1-QR* | CTTGCGGTTGGTCTTGTGC | *Ascl1-QR* | ATTTGACGTCGTTGGCGAGA |
| *Msx2-QF* | ACACCCTTCACCACATCCCA | *L1cam-QF* | GCTCCTCATCCTGCTCATCC |
| *Msx2-QR* | TTCCGCCTCTTGCAGTCTTT | *L1cam-QR* | TCTCCAGGGACCTGTACTCG |
| *Pax9-QF* | TATTCTGCGCAACAAGATCG | *Osr2-QF* | TCTTTACACATCCCGCTTCC |
| *Pax9-QR* | GGTGGTGTAGGCACCTTAGC | *Osr2-QR* | GGAAAGGTCATGAGGTCCAA |
| *Fgf10-QF* | TTTGAGCCATAGAGTTTCCCC | *Gapdh-F* | TGGAGCCAAAAGGGTCA |
| *Fgf10-QR* | CGGGACCAAGAATGAAGACTG | *Gapdh-R* | CTTCTGGGTGGCAGTGA |